

Supplementary Information for

Membrane destabilizing ionizable phospholipids for organ selective mRNA delivery and CRISPR/Cas gene editing

Shuai Liu,^{1,†} Qiang Cheng,^{1,†} Tuo Wei,¹ Xueliang Yu,¹ Lindsay T. Johnson¹, Lukas Farbiak¹, and Daniel J. Siegwart^{1,*}

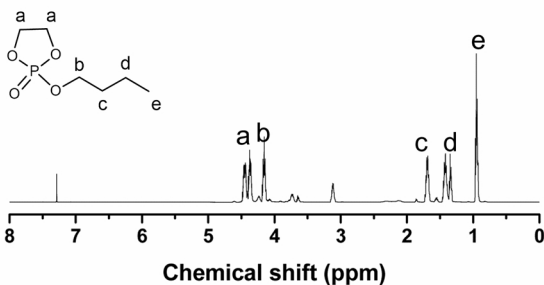
¹The University of Texas Southwestern Medical Center, Department of Biochemistry, Simmons Comprehensive Cancer Center, Dallas, United States. * Correspondence to: Daniel.Siegwart@UTSouthwestern.edu † These authors contributed equally to this work.

This PDF file includes:

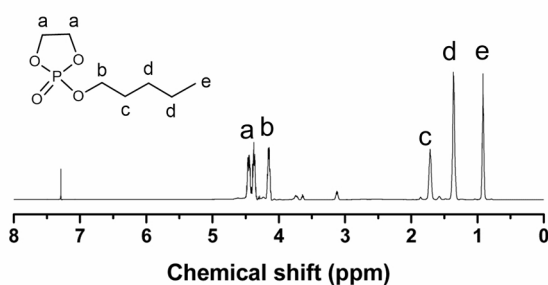
Supplementary Figures S1 to S32
Supplementary Tables S1 to S3
Supplementary Methods

Supplementary Figures

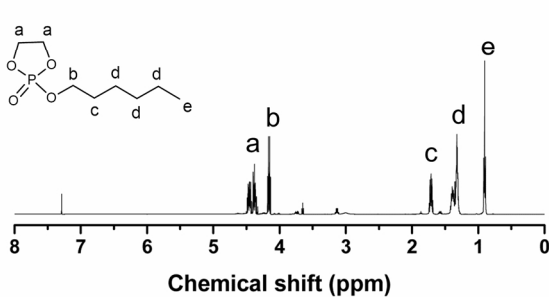
P4 Conversion yield 90.8%



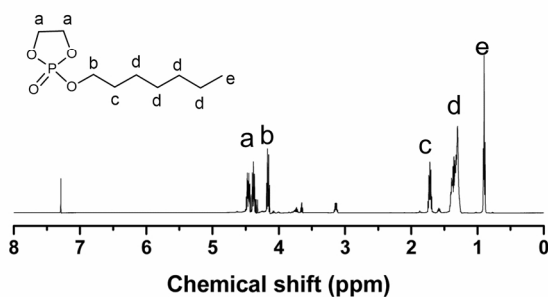
P5 Conversion yield 96.8%



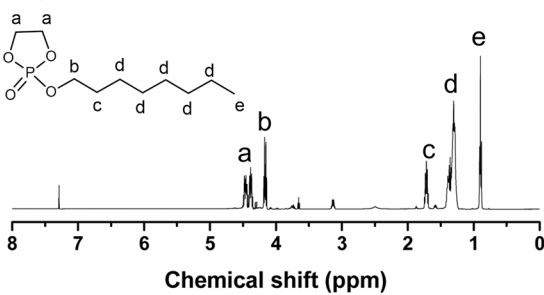
P6 Conversion yield 96.8%



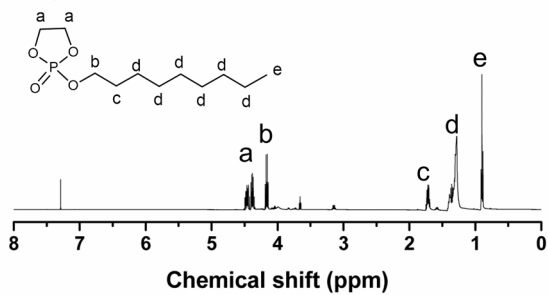
P7 Conversion yield 96.0%



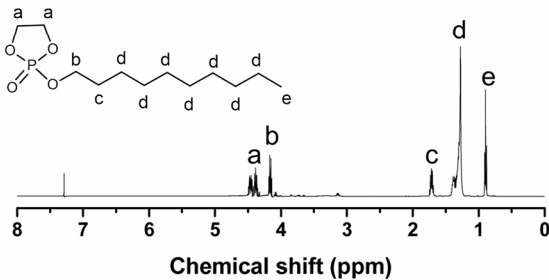
P8 Conversion yield 93.0%



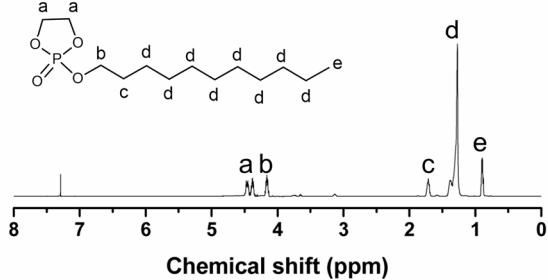
P9 Conversion yield 87.0%

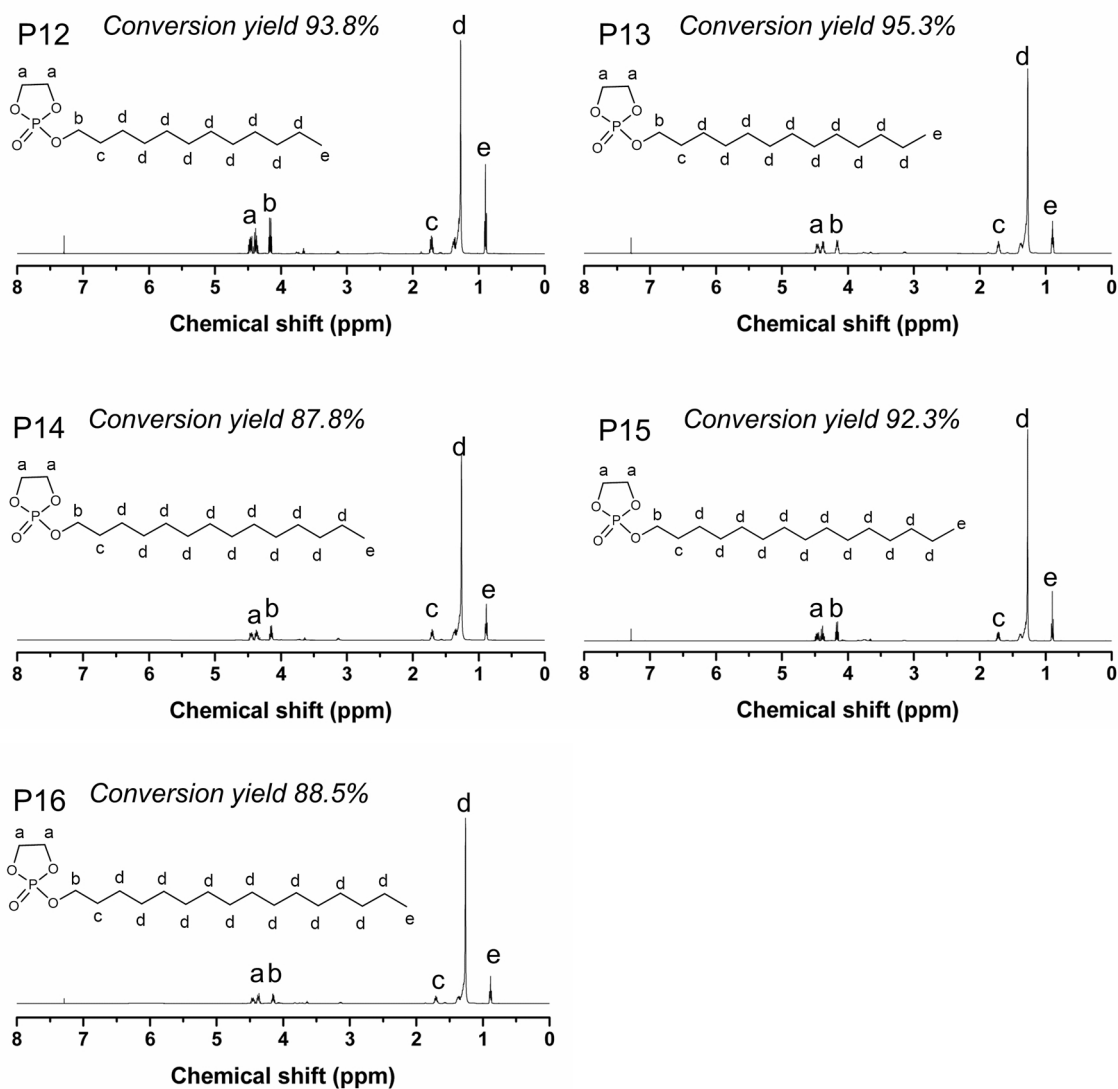


P10 Conversion yield 93.0%



P11 Conversion yield 95.3%



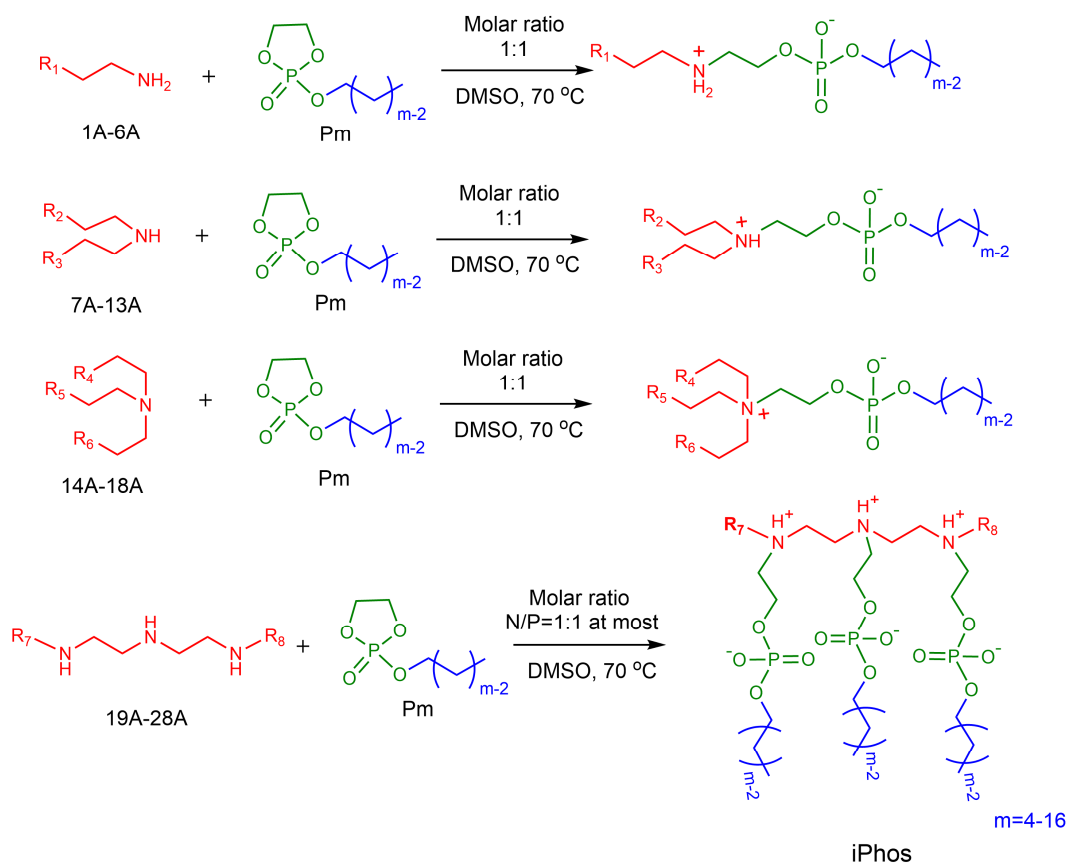


Supplementary Figure 1 ^1H NMR spectra of alkylated dioxaphospholane oxide molecules P4-P16 (CDCl_3). The conversion yields of corresponding alcohols to products were 90.8% (P4), 96.8% (P5), 96.8% (P6), 96.0% (P7), 93.0% (P8), 87.0% (P9), 93.0% (P10), 95.3% (P11), 93.8% (P12), 95.3% (P13), 87.8% (P14), 92.3% (P15), 88.5% (P16), respectively. The conversion yields were calculated from integrals of peak **a** (4H, $-\text{OCH}_2\text{CH}_2\text{O}-$ in Pm molecules) and peak **e** (3H, $-\text{CH}_2\text{CH}_2\text{CH}_3$ in both Pm and corresponding alcohol molecules).

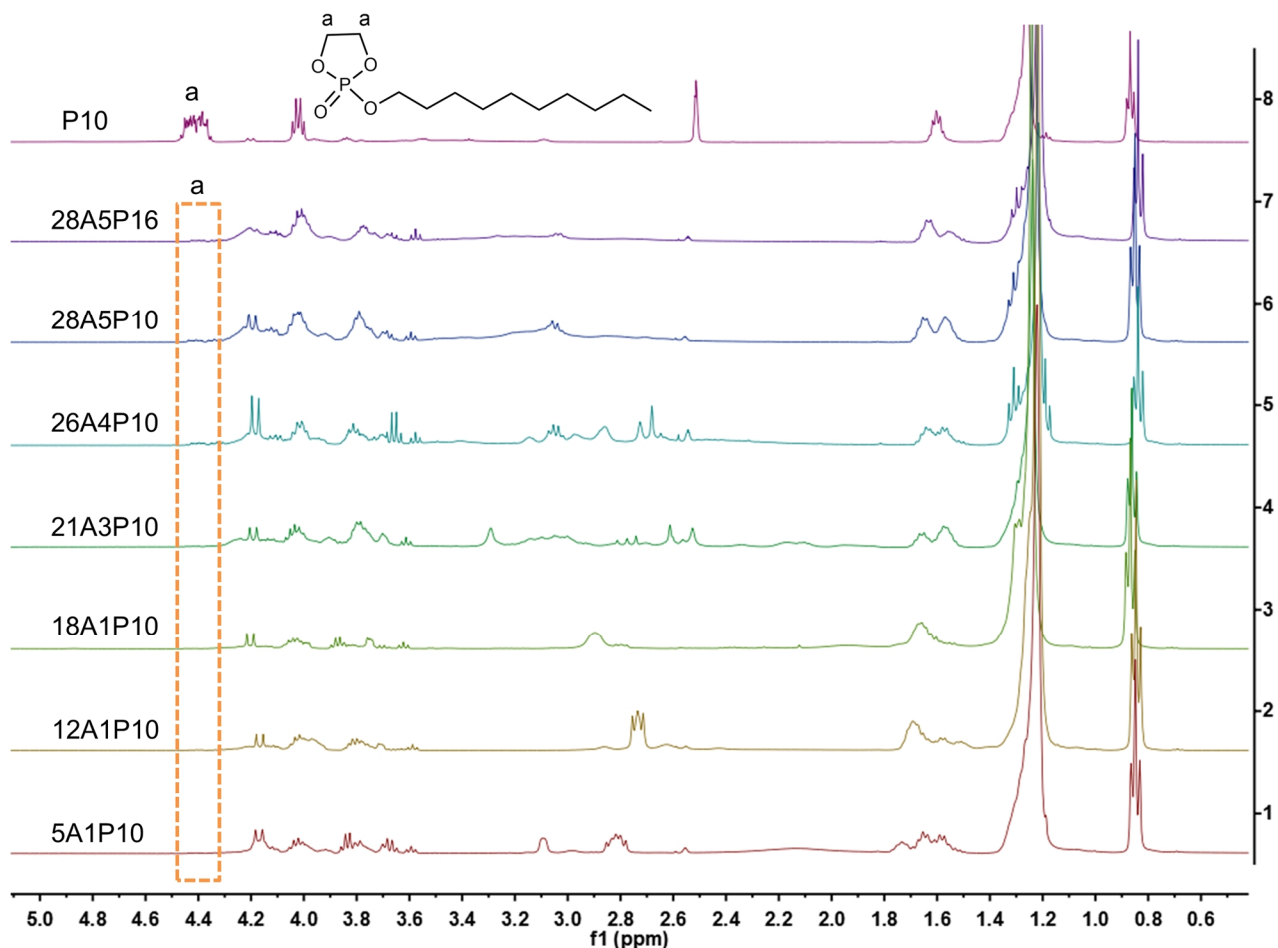
P4: ^1H NMR (CDCl_3 , ppm) δ 0.95 (t, 3H, $-\text{CH}_2\text{CH}_2\text{CH}_2\text{CH}_3$), 1.37 (m, 2H, $-\text{CH}_2\text{CH}_2\text{CH}_2\text{CH}_3$), 1.68 (m, 2H, $-\text{OCH}_2\text{CH}_2\text{CH}_2\text{CH}_3$), 4.16 (m, 2H, $-\text{OCH}_2\text{CH}_2\text{CH}_2\text{CH}_3$), 4.40 (m, 4H, $-\text{OCH}_2\text{CH}_2\text{O}-$).

P5: ^1H NMR (CDCl_3 , ppm) δ 0.92 (t, 3H, $-\text{CH}_2\text{CH}_2\text{CH}_2\text{CH}_3$), 1.36 (m, 4H, $-\text{CH}_2\text{CH}_2\text{CH}_2\text{CH}_3$), 1.71 (m, 2H, $-\text{OCH}_2\text{CH}_2\text{CH}_2\text{CH}_2\text{CH}_3$), 4.16 (m, 2H, $-\text{OCH}_2\text{CH}_2\text{CH}_2\text{CH}_2\text{CH}_3$), 4.40 (m, 4H, $-\text{OCH}_2\text{CH}_2\text{O}-$).

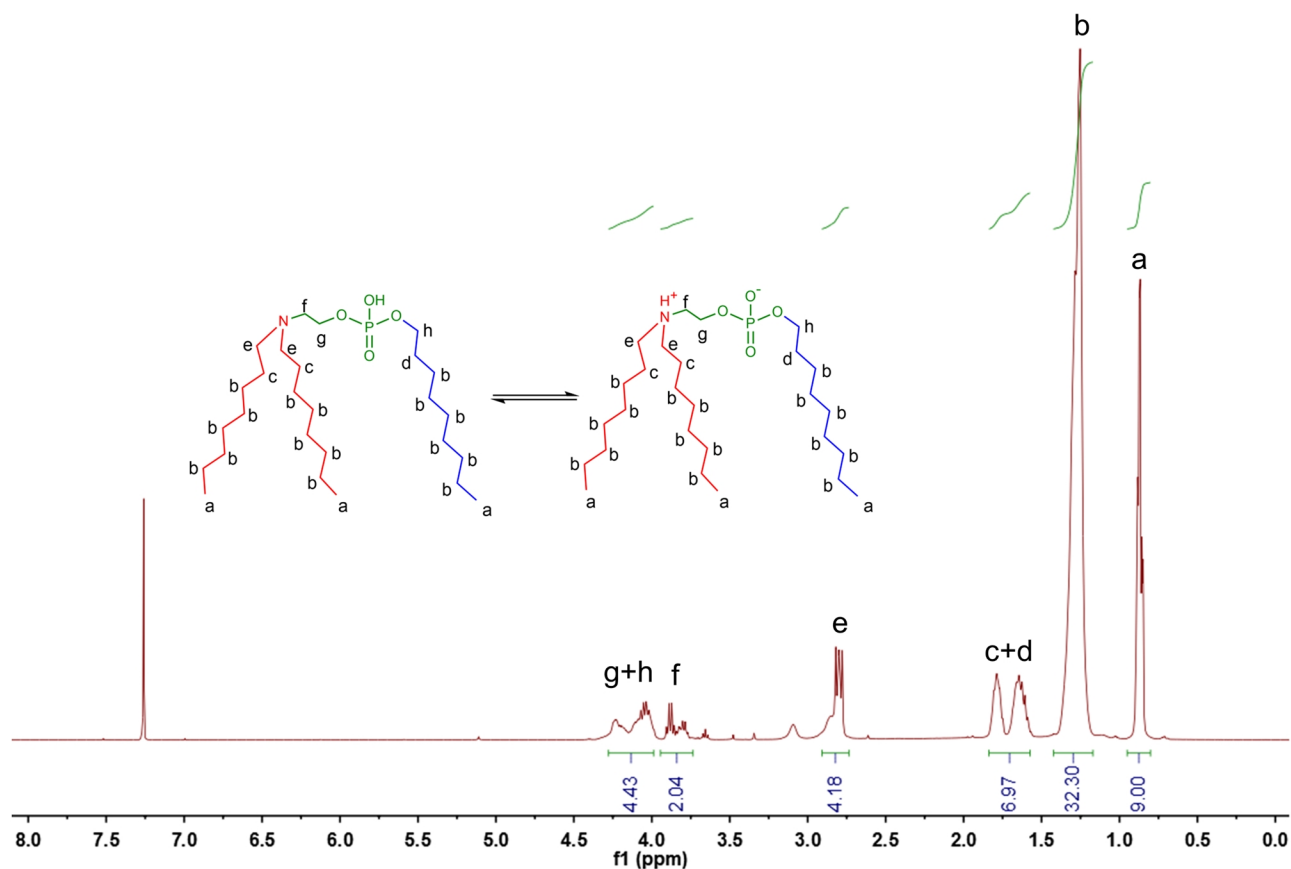
P6: ^1H NMR (CDCl_3 , ppm) δ 0.90 (t, 3H, $-\text{CH}_2\text{CH}_2\text{CH}_2\text{CH}_3$), 1.32 (m, 6H, $-\text{CH}_2\text{CH}_2\text{CH}_2\text{CH}_2\text{CH}_3$), 1.72 (m, 2H, $-\text{OCH}_2\text{CH}_2\text{CH}_2\text{CH}_2\text{CH}_2\text{CH}_3$), 4.16 (m, 2H, $-\text{OCH}_2\text{CH}_2\text{CH}_2\text{CH}_2\text{CH}_2\text{CH}_3$), 4.42 (m, 4H, $-\text{OCH}_2\text{CH}_2\text{O}-$).



Supplementary Figure 2 | iPhos syntheses using different amine starting materials. Amines with one primary, secondary, or tertiary amine group introduced a single zwitterion. Amines with several amine groups introduced multiple zwitterions.

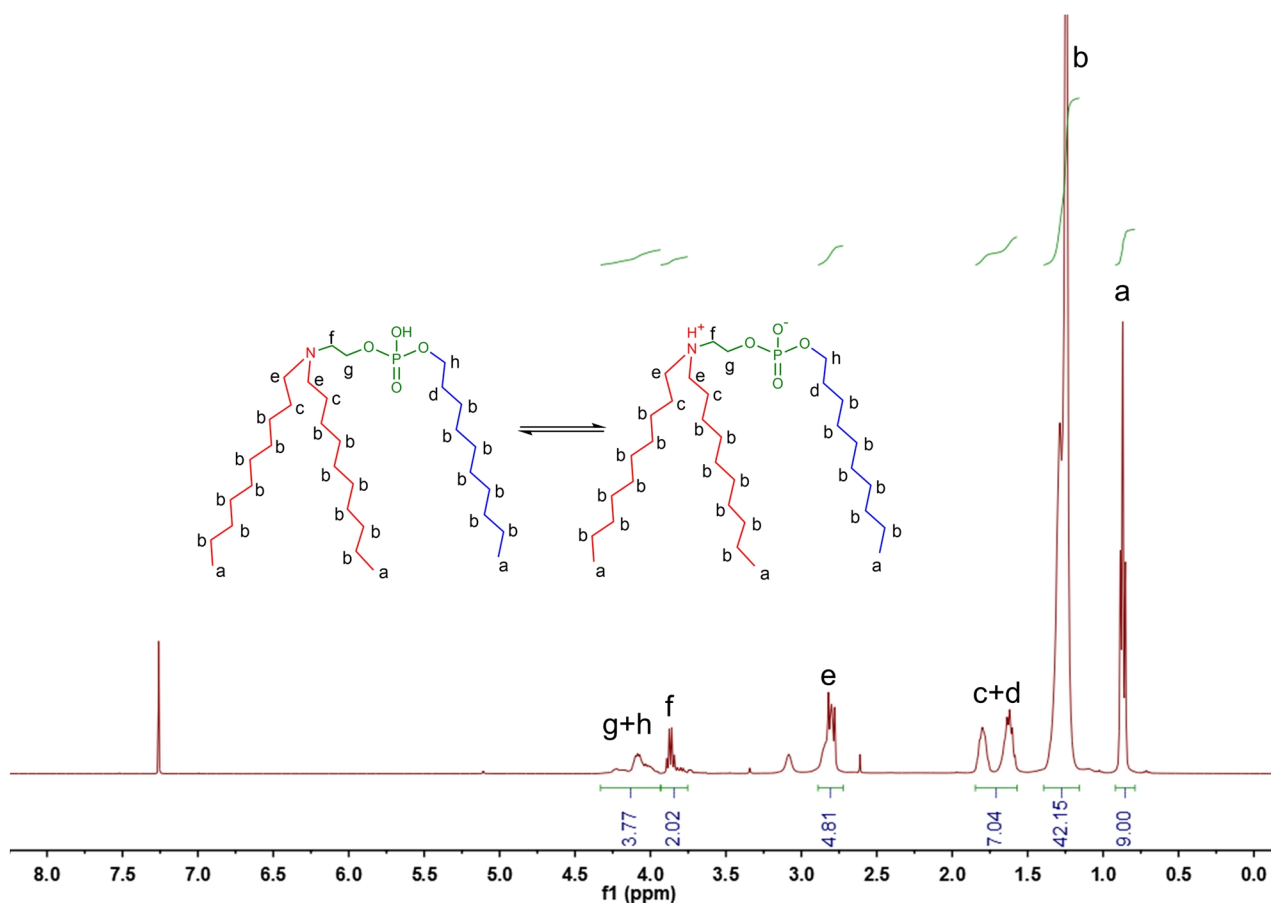


Supplementary Figure 3 | ¹H NMR spectra of P10 (DMSO-d6) and selected iPhos (CDCl₃). The spectrum of P10 was recorded after stirring in DMSO-d6 at 70 °C and it remained almost unchanged. For the iPhos, the reaction occurred in DMSO-d6 at 70 °C for 3 days and the disappeared peak **a** (4.4 ppm) of methylene group post reaction indicated that almost all P10 had been consumed by the amine groups. In addition, less active P16 could also react completely with amines.



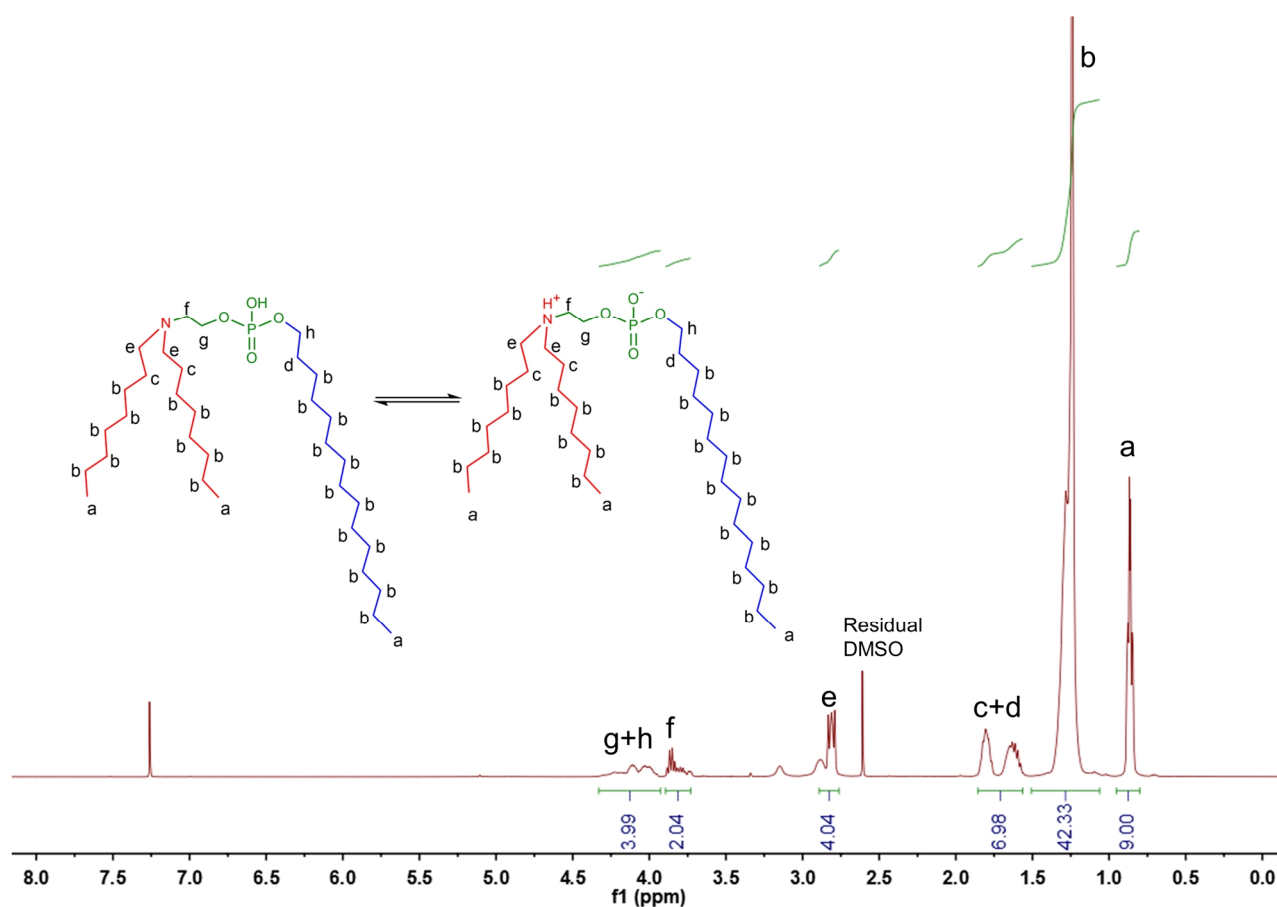
Supplementary Figure 5 | ^1H NMR spectrum of 9A1P9 in CDCl_3 .

^1H NMR (CDCl_3 , ppm) δ 0.87 (m, 9H, $-\text{CH}_2\text{CH}_2\text{CH}_2\text{CH}_3$), 1.25 (m, 32H, $-\text{OCH}_2\text{CH}_2(\text{CH}_2)_6\text{CH}_3$ and $-\text{N}(\text{CH}_2\text{CH}_2\text{CH}_2\text{CH}_2\text{CH}_2\text{CH}_2\text{CH}_3)_2$), 1.55-1.84 (m, 6H, $-\text{OCH}_2\text{CH}_2(\text{CH}_2)_6\text{CH}_3$ and $-\text{N}(\text{CH}_2\text{CH}_2\text{CH}_2\text{CH}_2\text{CH}_2\text{CH}_2\text{CH}_3)_2$), 2.80 (m, 4H, $-\text{N}(\text{CH}_2\text{CH}_2\text{CH}_2\text{CH}_2\text{CH}_2\text{CH}_2\text{CH}_3)_2$), 3.87 (m, 2H, $-\text{NCH}_2\text{CH}_2\text{O}-$), 3.96-4.28 (m, 4H, $-\text{NCH}_2\text{CH}_2\text{O}-$ and $-\text{OCH}_2\text{CH}_2(\text{CH}_2)_6\text{CH}_3$). ^{13}C NMR (CDCl_3 , ppm) δ 14.08, 14.10, 22.61, 22.66, 26.00, 27.00, 27.03, 29.16, 29.22, 29.25, 29.32, 29.45, 29.49, 29.62, 31.73, 31.77, 47.72. ^{31}P NMR (CDCl_3 , ppm) δ -0.91, 0.94. Mass calculated m/z 491.4, found $[\text{M}+\text{H}]^+$ (LC-MS direct injection) m/z 492.4.



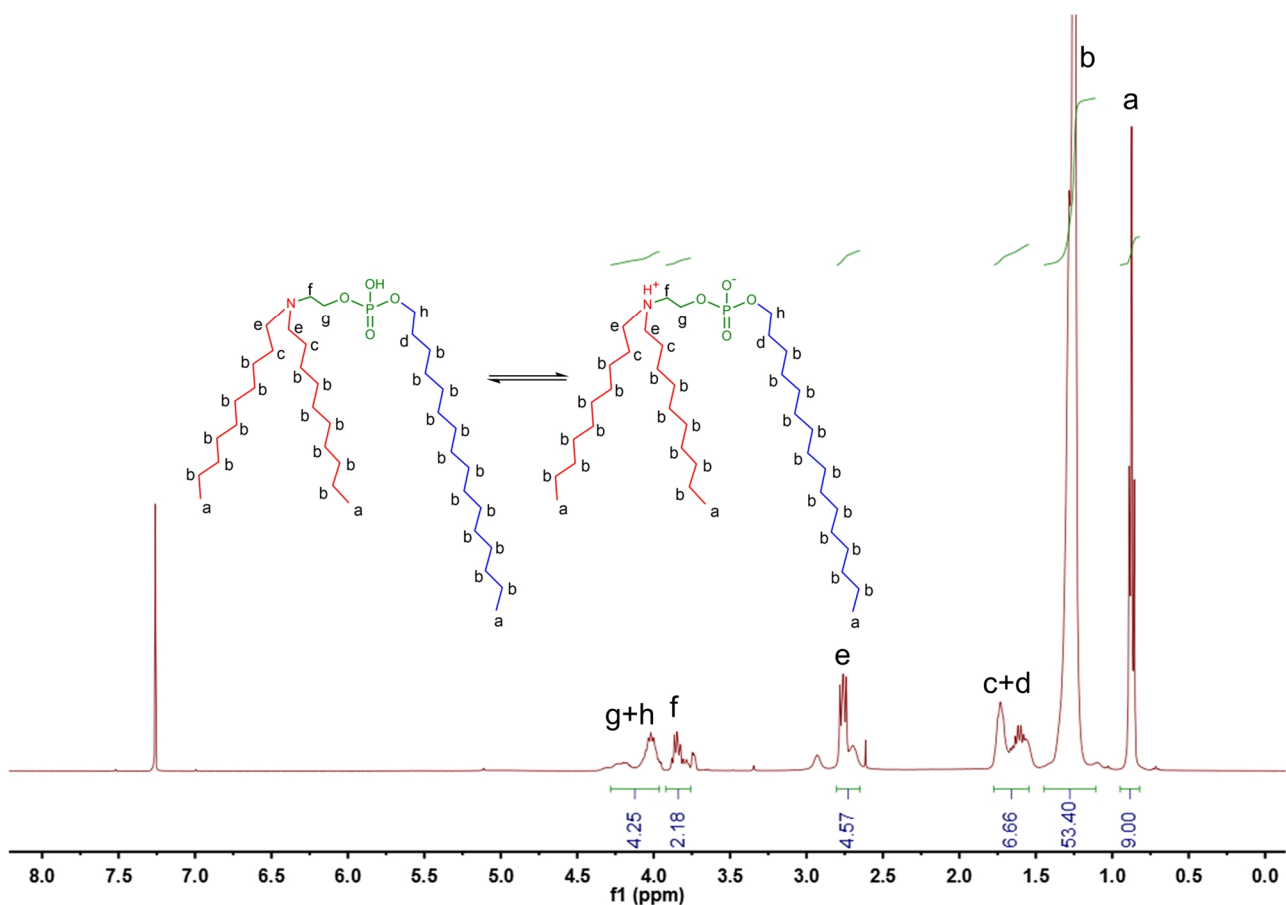
Supplementary Figure 6 | ^1H NMR spectrum of 10A1P10 in CDCl_3 .

^1H NMR (CDCl_3 , ppm) δ 0.87 (t, 9H, $-\text{CH}_2\text{CH}_2\text{CH}_2\text{CH}_3$), 1.25 (m, 42H, $-\text{OCH}_2\text{CH}_2(\text{CH}_2)_7\text{CH}_3$ and $-\text{N}(\text{CH}_2\text{CH}_2\text{CH}_2\text{CH}_2\text{CH}_2\text{CH}_2\text{CH}_2\text{CH}_2\text{CH}_3)_2$), 1.57-1.85 (m, 6H, $-\text{OCH}_2\text{CH}_2(\text{CH}_2)_7\text{CH}_3$ and $-\text{N}(\text{CH}_2\text{CH}_2\text{CH}_2\text{CH}_2\text{CH}_2\text{CH}_2\text{CH}_2\text{CH}_2\text{CH}_3)_2$), 2.81 (m, 4H, $-\text{N}(\text{CH}_2\text{CH}_2\text{CH}_2\text{CH}_2\text{CH}_2\text{CH}_2\text{CH}_2\text{CH}_2\text{CH}_2\text{CH}_3)_2$), 3.87 (m, 2H, $-\text{NCH}_2\text{CH}_2\text{O}-$), 3.94-4.30 (m, 4H, $-\text{NCH}_2\text{CH}_2\text{O}-$ and $-\text{OCH}_2\text{CH}_2(\text{CH}_2)_7\text{CH}_3$). ^{13}C NMR (CDCl_3 , ppm) δ 14.10, 22.68, 26.00, 27.01, 27.05, 29.28, 29.32, 29.35, 29.46, 29.51, 29.57, 29.62, 31.86, 31.89, 47.61. ^{31}P NMR (CDCl_3 , ppm) δ -1.08, 0.86. Mass calculated m/z 561.5, found $[\text{M}+\text{H}]^+$ (LC-MS direct injection) m/z 563.6.



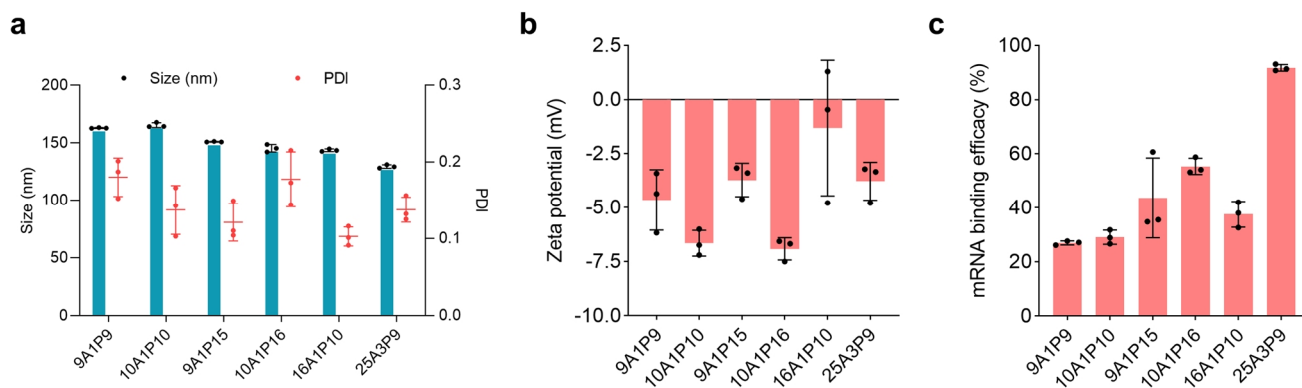
Supplementary Figure 7 | ^1H NMR spectrum of 9A1P15 in CDCl_3 . A little DMSO was remained in the product by column flash chromatography, but it would not influence 9A1P15 effect.

^1H NMR (CDCl_3 , ppm) δ 0.86 (m, 9H, $-\text{CH}_2\text{CH}_2\text{CH}_2\text{CH}_3$), 1.24 (m, 44H, $-\text{OCH}_2\text{CH}_2(\text{CH}_2)_{12}\text{CH}_3$ and $-\text{N}(\text{CH}_2\text{CH}_2\text{CH}_2\text{CH}_2\text{CH}_2\text{CH}_2\text{CH}_2\text{CH}_3)_2$), 1.56-1.86 (m, 6H, $-\text{OCH}_2\text{CH}_2(\text{CH}_2)_{12}\text{CH}_3$ and $-\text{N}(\text{CH}_2\text{CH}_2\text{CH}_2\text{CH}_2\text{CH}_2\text{CH}_2\text{CH}_2\text{CH}_3)_2$), 2.81 (m, 4H, $-\text{N}(\text{CH}_2\text{CH}_2\text{CH}_2\text{CH}_2\text{CH}_2\text{CH}_2\text{CH}_2\text{CH}_3)_2$), 3.86 (m, 2H, $-\text{NCH}_2\text{CH}_2\text{O}-$), 3.94-4.30 (m, 4H, $-\text{NCH}_2\text{CH}_2\text{O}-$ and $-\text{OCH}_2\text{CH}_2(\text{CH}_2)_{12}\text{CH}_3$). ^{13}C NMR (CDCl_3 , ppm) δ 14.07, 14.11, 22.61, 22.68, 25.87, 26.96, 27.01, 29.16, 29.19, 29.23, 29.35, 29.47, 29.65, 29.70, 31.72, 31.76, 47.49. ^{31}P NMR (CDCl_3 , ppm) δ -0.95, 0.80. Mass calculated m/z 575.5, found $[\text{M}+\text{H}]^+$ (LC-MS direct injection) m/z 576.6.

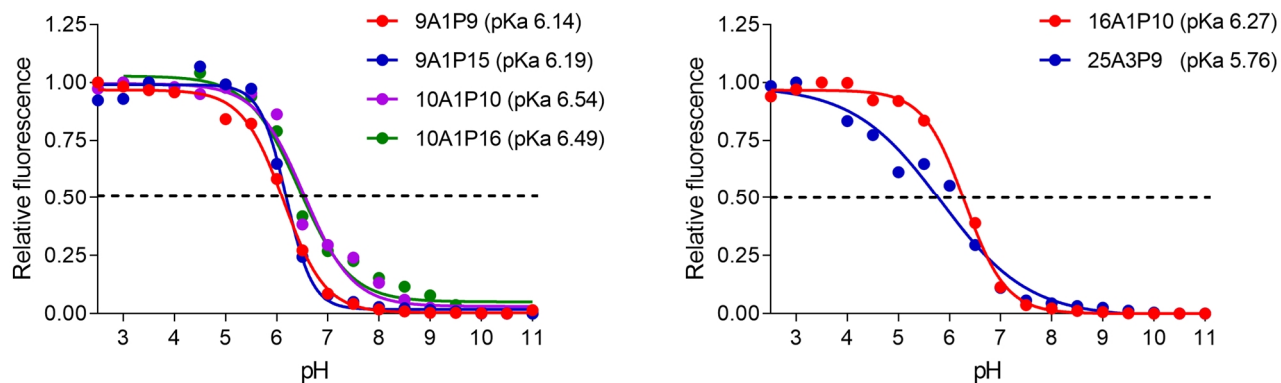


Supplementary Figure 8 | ¹H NMR spectrum of 10A1P16 in CDCl₃.

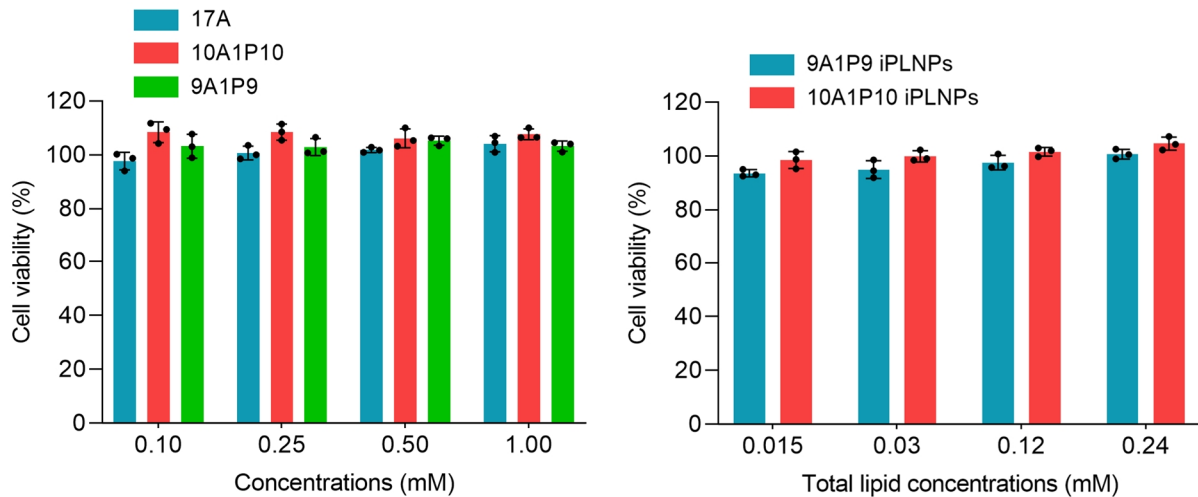
¹H NMR (CDCl₃, ppm) δ 0.87 (t, 9H, -CH₂CH₂CH₂CH₃), 1.25 (m, 54H, -OCH₂CH₂(CH₂)₁₃CH₃ and -N(CH₂CH₂CH₂CH₂CH₂CH₂CH₂CH₂CH₂CH₃)₂), 1.54-1.78 (m, 6H, -OCH₂CH₂(CH₂)₁₃CH₃ and -N(CH₂CH₂CH₂CH₂CH₂CH₂CH₂CH₂CH₂CH₃)₂), 2.76 (m, 4H, -N(CH₂CH₂CH₂CH₂CH₂CH₂CH₂CH₂CH₂CH₃)₂), 3.85 (m, 2H, -NCH₂CH₂O-), 3.95-4.28 (m, 4H, -NCH₂CH₂O- and -OCH₂CH₂(CH₂)₁₃CH₃). ¹³C NMR (CDCl₃, ppm) δ 14.11, 22.68, 25.91, 27.10, 27.20, 29.31, 29.34, 29.56, 29.59, 29.64, 29.66, 29.72, 31.88, 31.91, 47.78. ³¹P NMR (CDCl₃, ppm) δ -1.00, 0.76. Mass calculated m/z 645.6, found [M+H]⁺ (LC-MS direct injection) m/z 646.6.



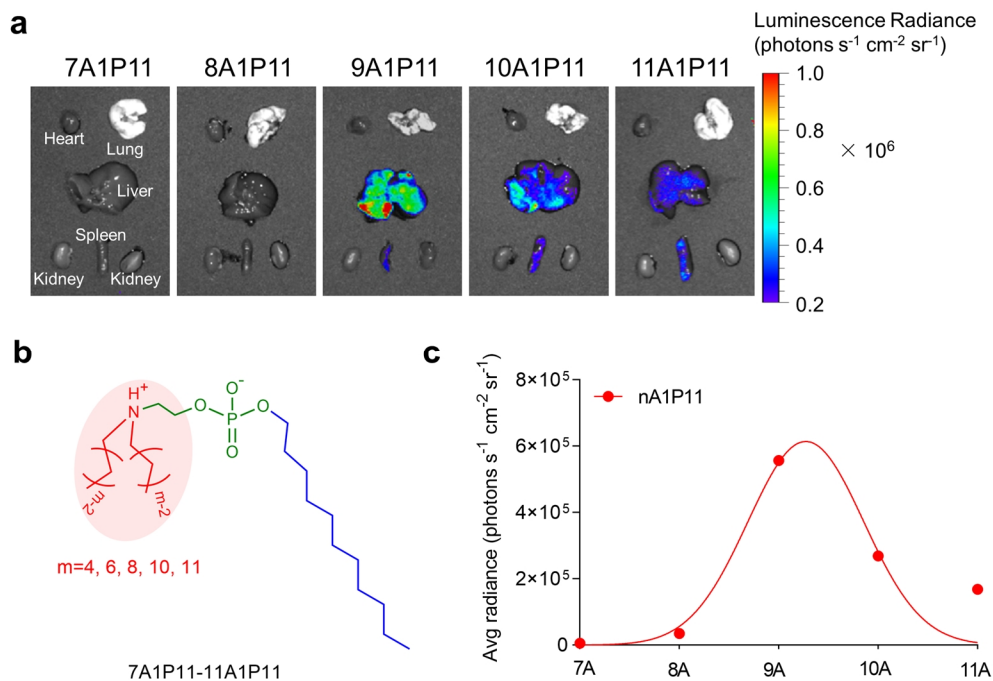
Supplementary Figure 9 | Characterization of selected iPLNPs. Particle size and polydispersity Index (PDI) (a), zeta potential (b), and mRNA binding efficacy (c) of selected iPLNPs were assayed. 9A1P9, 10A1P10, 9A1P15 and 10A1P16 were purified and their iPLNPs showed sizes around 150 nm. All data are presented as mean \pm s.d. (n = 3 biologically independent samples).



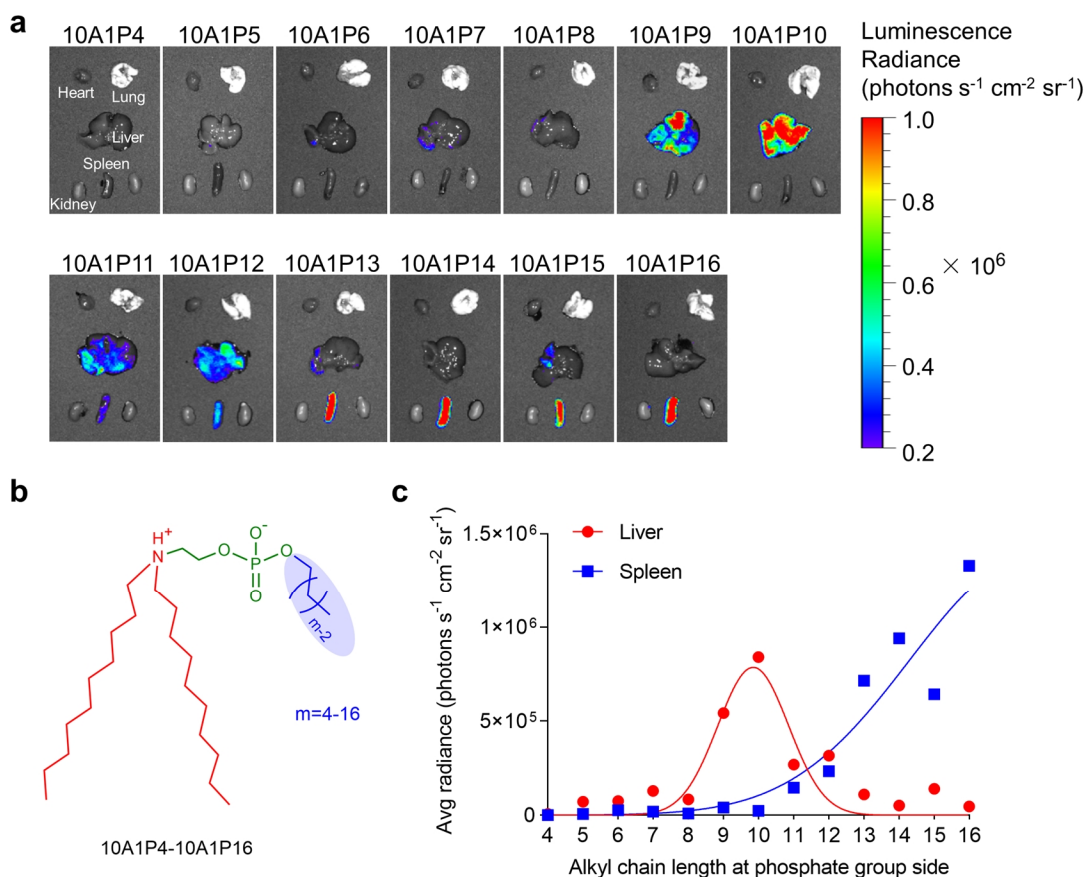
Supplementary Figure 10 | pKa of selected iPLNPs.



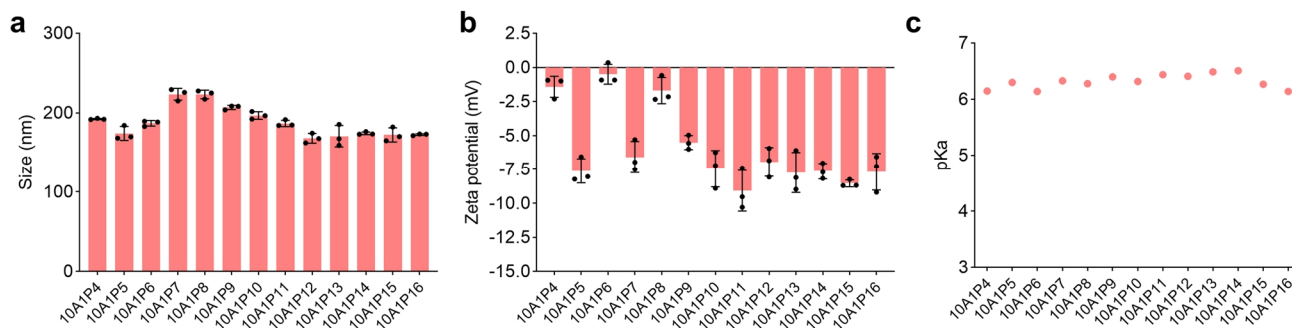
Supplementary Figure 11 | Cell viability of iPhos lipids and iPLNPs in IGROV1 cells. The concentrations and incubation time were the same as that used in the hemolysis assays. Data are presented as mean \pm s.d. (n = 3 biologically independent samples).



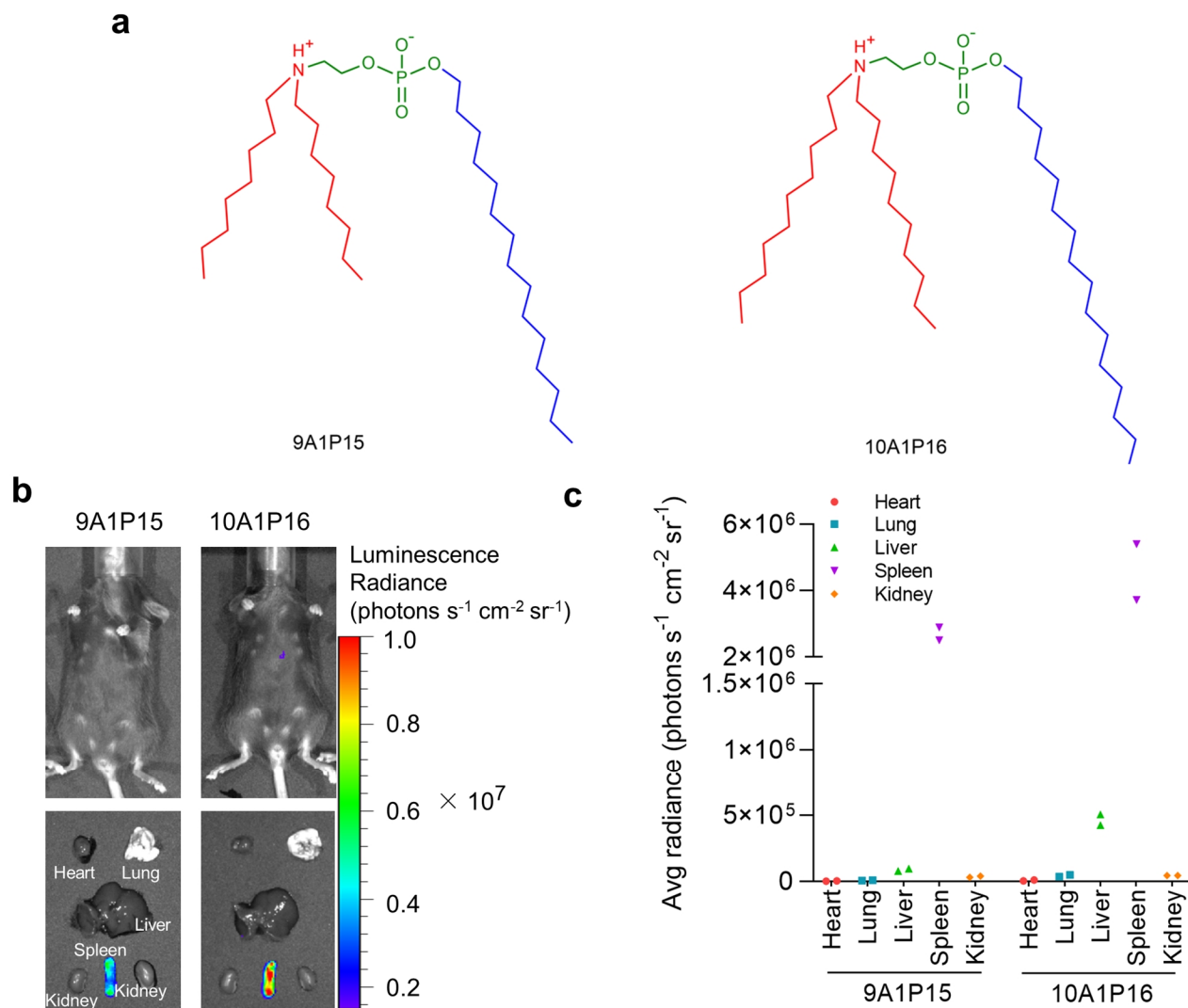
Supplementary Figure 12 | Different tail lengths at amine group side of iPhos influenced *in vivo* mRNA expression efficacy. **a**, Bioluminescence imaging of various organs 6 h post injection. C57BL/6 mice were IV injected by iPLNPs at 0.1 mg kg^{-1} FLuc mRNA and luminescence was quantified 6 h post injection. **b**, Structures of 7A1P11-11A1P11. **c**, Effect of alkyl chain length at amine group side on mRNA delivery efficacy *in vivo*. Too short (4-6) and too long (>10) carbon lengths both mediated decreased efficacy in liver. Eight and ten carbon lengths trended to show high FLuc mRNA expression.



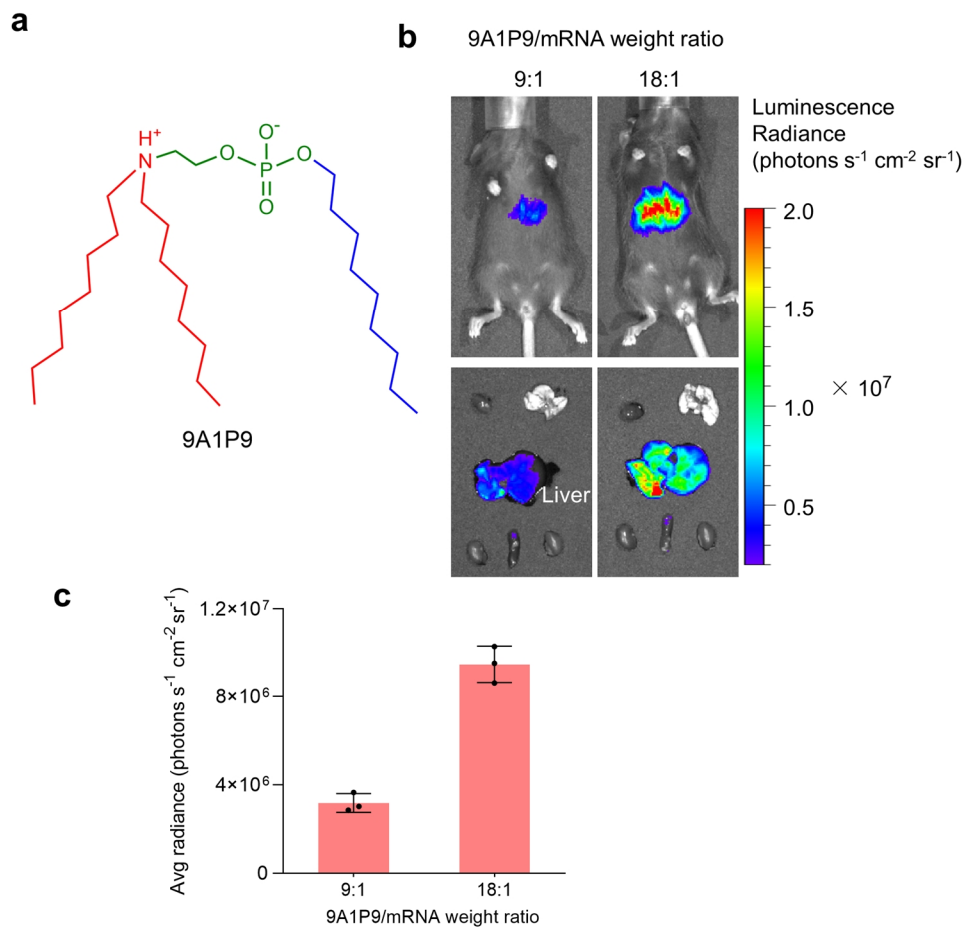
Supplementary Figure 13 | Different tail lengths at phosphate group side of iPhos influenced organ selective mRNA expression. **a**, Bioluminescence imaging of various organs 6 h post injection. C57BL/6 mice were IV injected by iPLNPs at 0.1 mg kg⁻¹ FLuc mRNA. **b**, Structures of 10A1P4-10A1P16. **c**, Effect of alkyl chain length at phosphate group side on organ selectivity. Short carbon lengths (4-8) showed no efficacy *in vivo*. Nine and ten carbon lengths trended to mediate high Fluc mRNA expression mainly in liver. Interestingly, longer carbon lengths (13-16) changed the majority of Fluc mRNA expression to spleen.



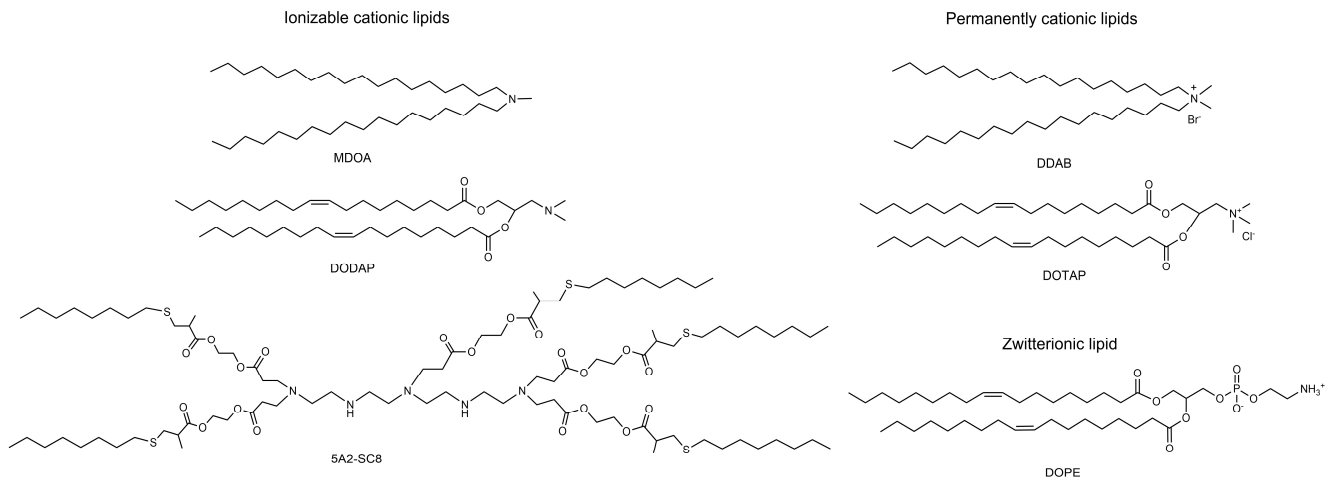
Supplementary Figure 14 | Characterization of iPLNPs. Particle size (**a**), zeta potential (**b**) and pKa (**c**) of 10A1P4-10A1P16 iPLNPs were assayed. 10A1P4-10A1P16 iPLNPs were generally negatively charged and showed sizes around 200 nm. These nanoparticles showed pKa from 6.0 to 6.5. Data in **a** and **b** are presented as mean \pm s.d. (n = 3 biologically independent samples).



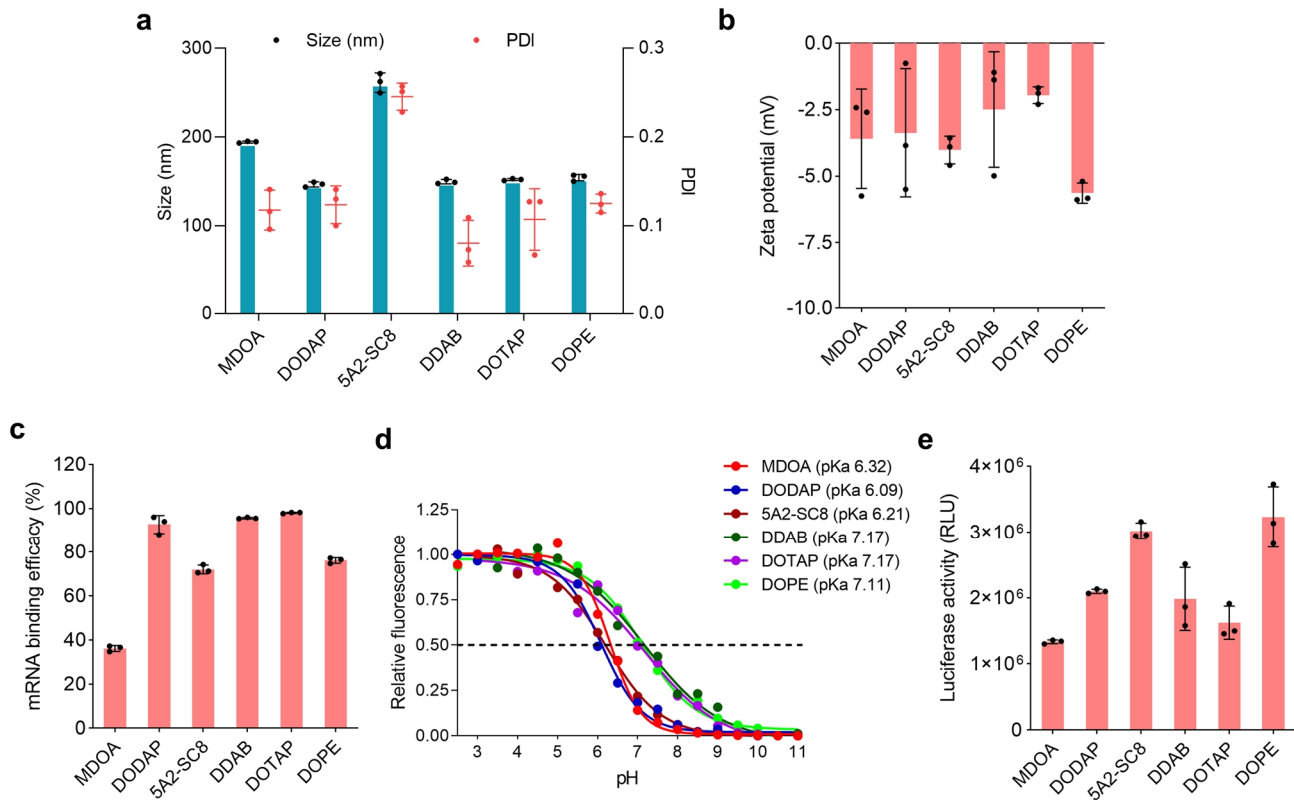
Supplementary Figure 15 | *In vivo* evaluation of 9A1P15 and 10A1P16 iPLNPs. **a**, Structures of 9A1P15 and 10A1P16 in acidic endosomal environment. **b**, C57BL/6 mice were IV injected by iPLNPs at 0.25 mg kg^{-1} FLuc mRNA and luminescence was quantified 6 h post injection. **c**, Quantification of luciferase expression in various organs was recorded by average radiance. 9A1P15/mRNA weight ratio of 10:1 and 10A1P16/mRNA weight ratio of 11.5:1 (molar ratio 11622:1) were used. iPhos: MDOA: chol: DMG-PEG2000 molar ratio was fixed at 25:30:30:1. Data are presented as mean \pm s.d. ($n = 2$ biologically independent mice).



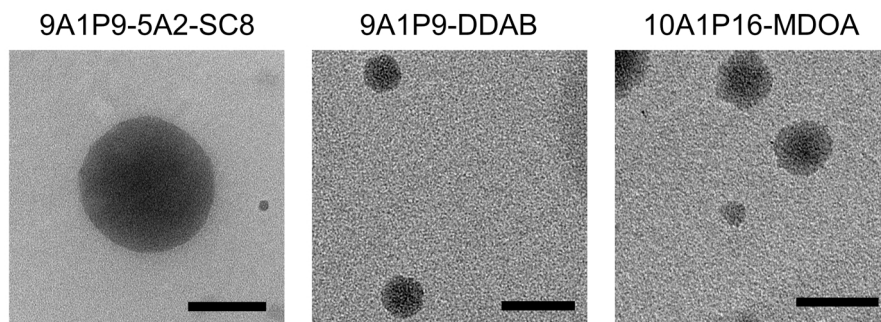
Supplementary Figure 16 | 9A1P9/mRNA weight ratio affected *in vivo* efficacy. **a**, Structure of 9A1P9 in acidic endosomal environment. **b**, 9A1P9/mRNA weight ratio of 9:1 (molar ratio 11622:1) and 18:1 (molar ratio 23244:1) were evaluated. iPhos: MDOA: chol: DMG-PEG2000 molar ratio was fixed at 25:30:30:1. C57BL/6 mice were IV injected by iPLNPs at 0.25 mg kg⁻¹ FLuc mRNA and luminescence was quantified 6 h post injection. **c**, Quantification of luciferase expression in liver was recorded by average radiance. Data are presented as mean ± s.d. (n = 3 biologically independent mice).



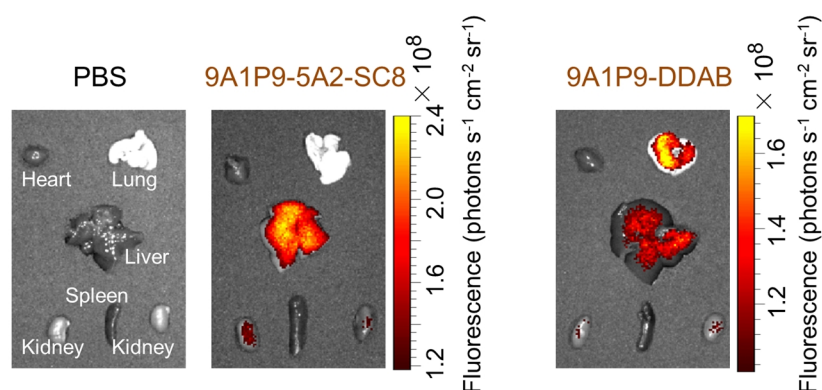
Supplementary Figure 17 | Structures of the helper lipids. Ionizable cationic lipids included MDOA, DODAP, and 5A2-SC8. Permanently cationic lipids included DDAB and DOTAP. Zwitterionic lipid DOPE was used as helper lipid.



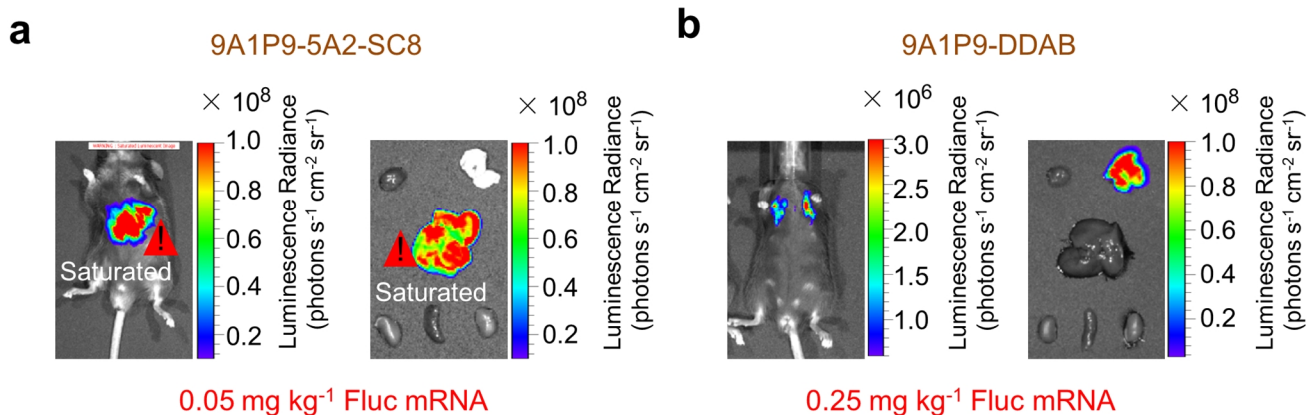
Supplementary Figure 18 | Characterization of 9A1P9 iPLNPs with different helper lipids. Particle size, PDI (a), zeta potential (b), mRNA binding efficacy (c), pKa (d) and *in vitro* mRNA delivery efficacy (e) in IGROV-1 cells (25 ng mRNA) of 9A1P9 iPLNPs with different helper lipids. 9A1P9: MDOA (DODAP or 5A2-SC8): chol: DMG-PEG2000 (molar ratio) = 25:30:30:1. 9A1P9: DDAB (or DOTAP): chol: DMG-PEG2000 (molar ratio) = 60:30:40:0.4. 9A1P9: DOPE: chol: DMG-PEG2000 (molar ratio) = 55:30:45:0.2. For all the formulations, 9A1P9: mRNA (w/w) = 18:1. Data in a, b, c and e are presented as mean ± s.d. (n = 3 biologically independent samples).



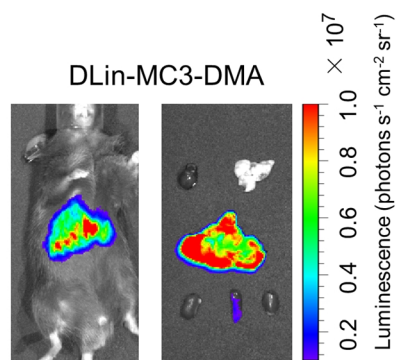
Supplementary Figure 19 | Representative TEM images of organ selective iPLNPs. 9A1P9-5A2-SC8, 9A1P9-DDAB, and 10A1P16-MDOA iPLNPs were prepared and imaged by TEM. They all exhibited a spherical morphology. This experiment was repeated three times independently with similar results. All scale bars = 100 nm.



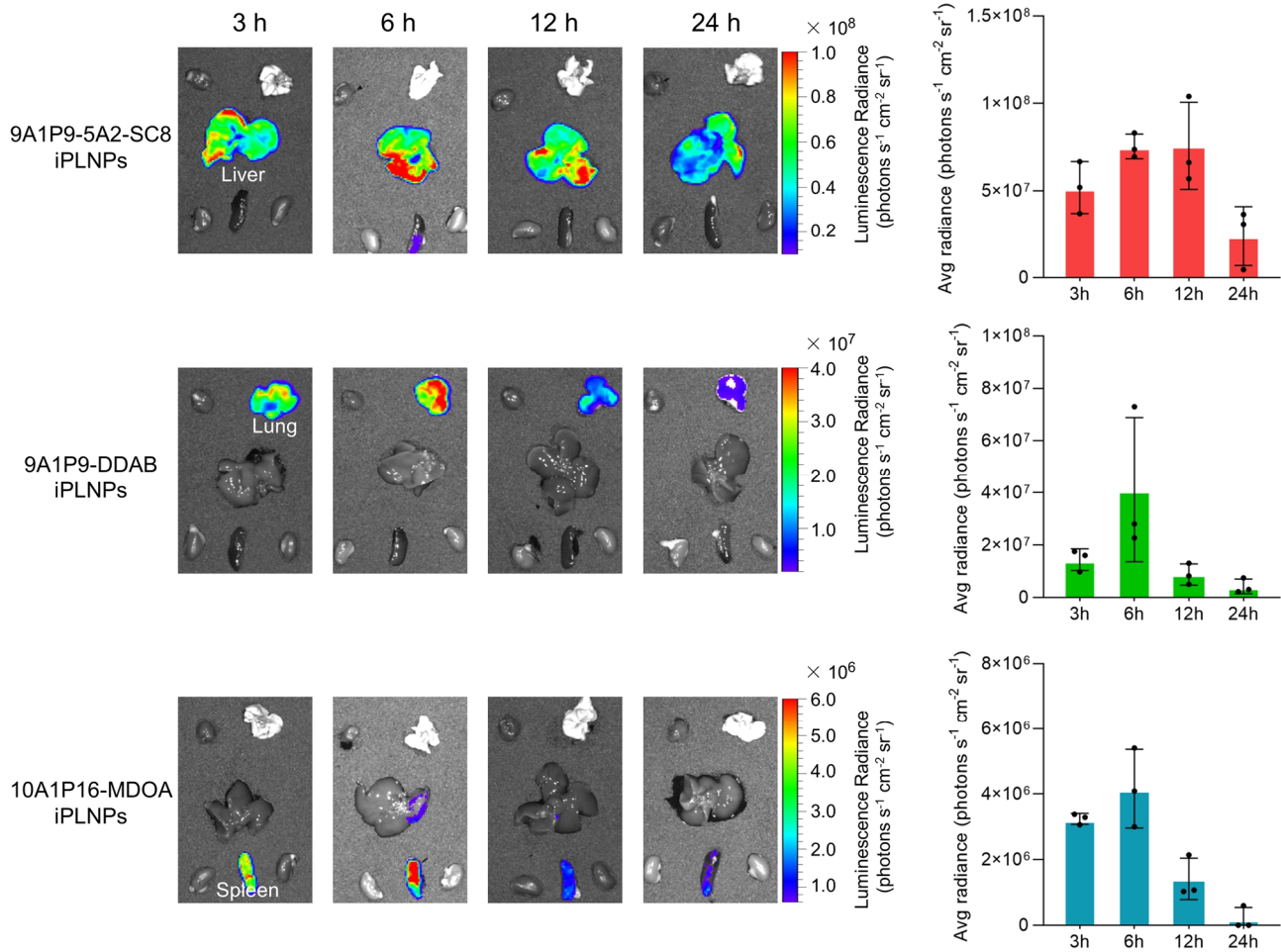
Supplementary Figure 20 | Representative images of organ distribution of Cy5-mRNA. C57BL/6 mice were IV injected by iPLNPs at 0.25 mg kg^{-1} Cy5-mRNA and imaged after 6 h. For iPLNP formulations, 9A1P9: 5A2-SC8: chol: DMG-PEG2000 molar ratio of 25:30:30:1 and 9A1P9: DDAB: chol: DMG-PEG2000 molar ratio of 60:30:40:0.4 were used. 9A1P9/mRNA (w/w) was fixed at 18/1. Data are from $n = 3$ biologically independent mice.



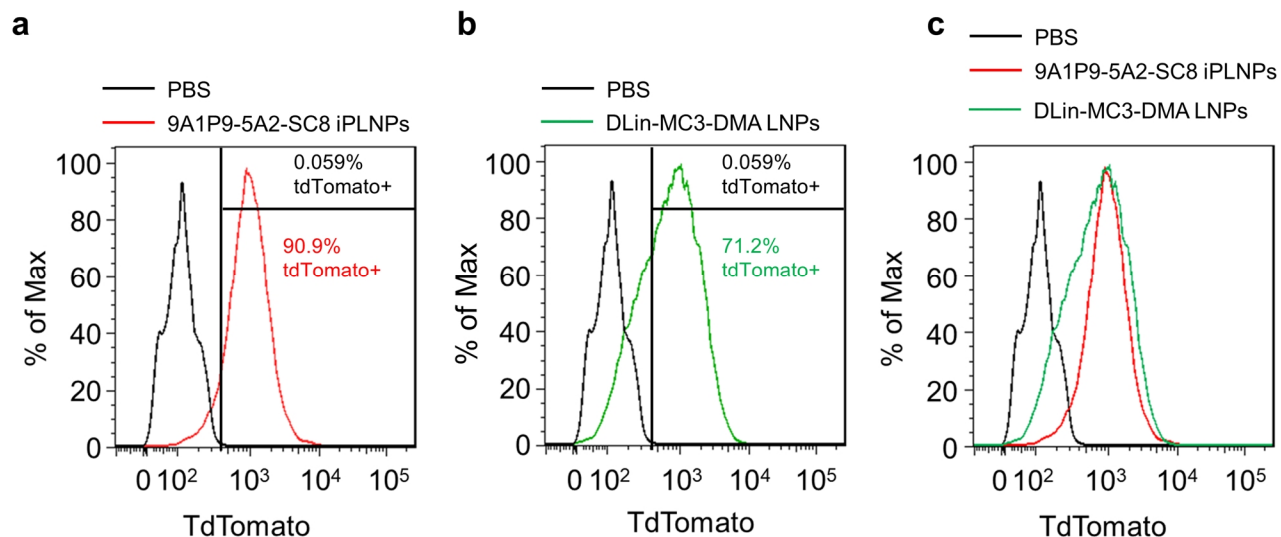
Supplementary Figure 21 | 9A1P9 iPLNPs showed organ selective mRNA expression. 9A1P9-5A2-SC8 (a) and 9A1P9-DDAB (b) iPLNPs showed high mRNA delivery efficacy in liver and lung, respectively. 9A1P9: 5A2-SC8: chol: DMG-PEG2000 (molar ratio) of 25:30:30:1 (Fluc mRNA, 0.05 mg kg⁻¹) and 9A1P9: DDAB: chol: DMG-PEG2000 (molar ratio) of 60:30:40:0.4 (Fluc mRNA, 0.25 mg kg⁻¹) were used. 9A1P9: mRNA weight ratio was fixed at 18:1. C57BL/6 mice were IV injected by iPLNPs and imaged after 6 h. Data are from n = 3 biologically independent mice.



Supplementary Figure 22 | DLin-MC3-DMA LNPs, showing effective mRNA delivery, are used as positive control. Images of luciferase expression were recorded 6 h post IV injection (Fluc mRNA, 0.05 mg kg⁻¹). The data are from n = 3 biologically independent mice.

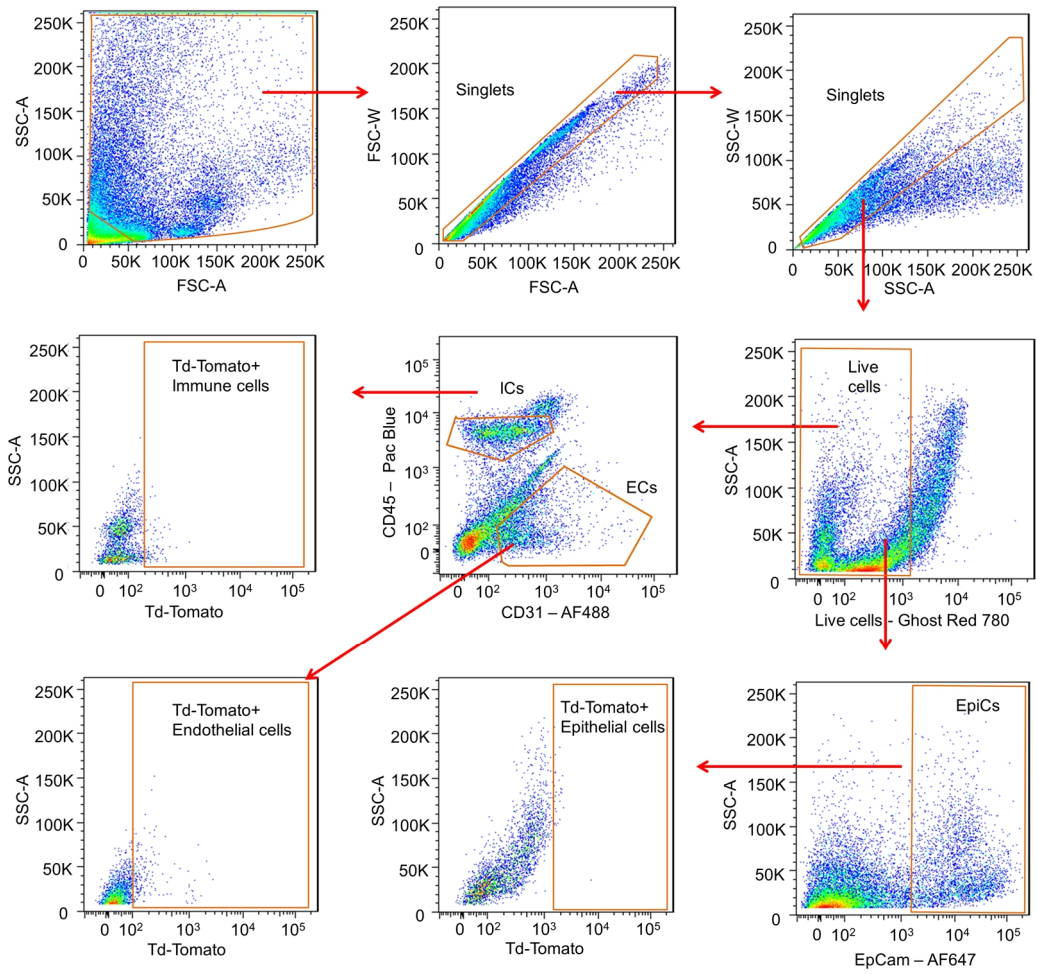


Supplementary Figure 23 | Kinetic analysis of Fluc protein expression by different organ selective iPLNPs. 9A1P9-5A2-SC8 (liver specific, 0.05 mg kg⁻¹ Fluc mRNA), 9A1P9-DDAB (lung specific, 0.25 mg kg⁻¹ Fluc mRNA) and 10A1P16-MDOA (spleen specific, 0.25 mg kg⁻¹ Fluc mRNA) iPLNPs were IV administrated to C57BL/6 mice. Organs were imaged after 3 h, 6 h, 12 h, and 24 h. Data are presented as mean ± s.d. (n = 3 biologically independent mice).

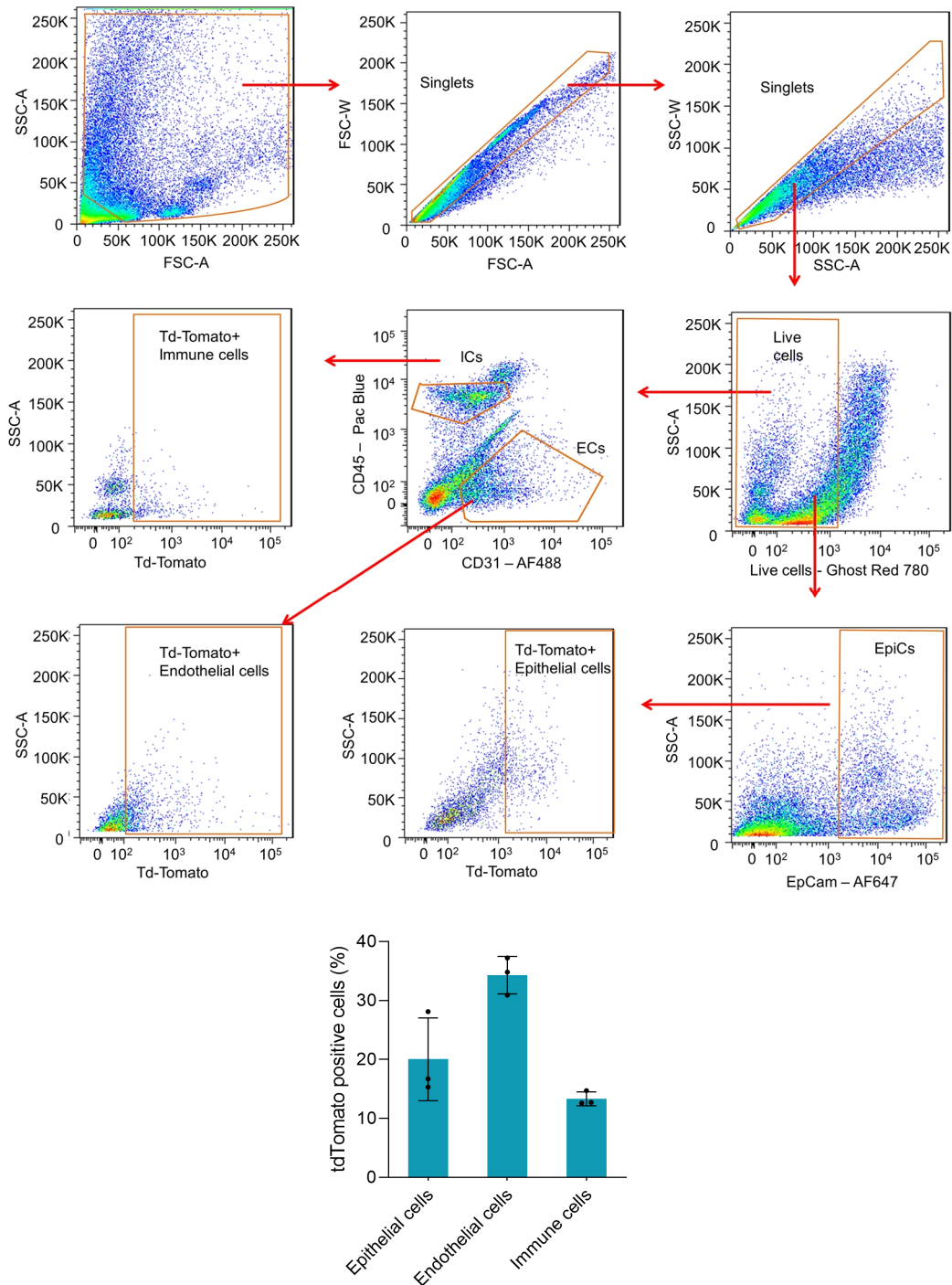


Supplementary Figure 24 | 9A1P9-5A2-SC8 iPLNPs achieved ~91% tdTomato editing in hepatocytes. **a**, 9A1P9-5A2-SC8 iPLNPs (Cre mRNA, 0.25 mg kg^{-1}) were IV administrated in Ai9 mice. After 48 h, hepatocytes were isolated and analyzed by flow cytometry. **b**, DLin-MC3-DMA LNPs (Cre mRNA, 0.25 mg kg^{-1}) were IV injected to Ai9 mice. After 48 h, hepatocytes were isolated and analyzed by flow cytometry. **c**, Merged results of 9A1P9-5A2-SC8 iPLNPs and DLin-MC3-DMA LNPs. All data are from $n = 3$ biologically independent mice.

PBS (lung)

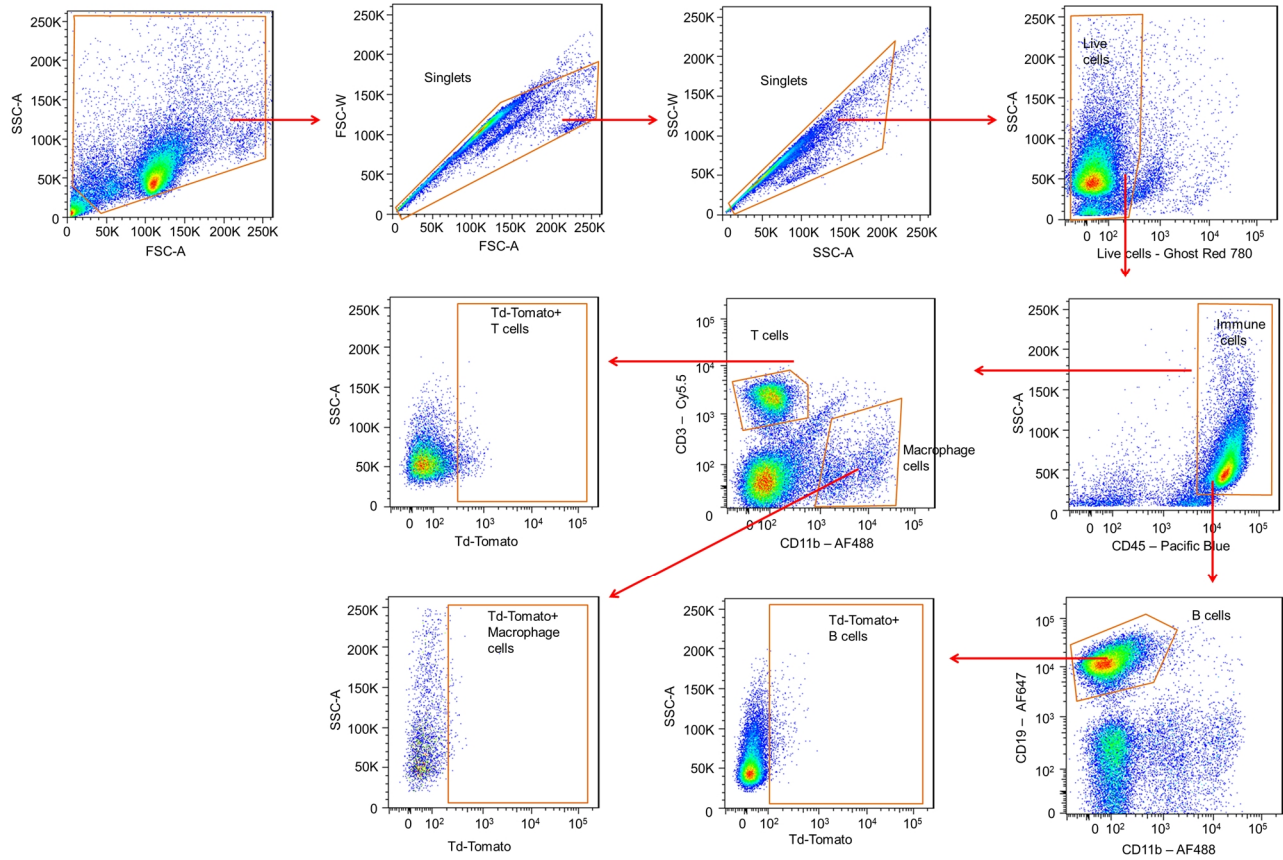


9A1P9-DDAB iPLNPs (lung)

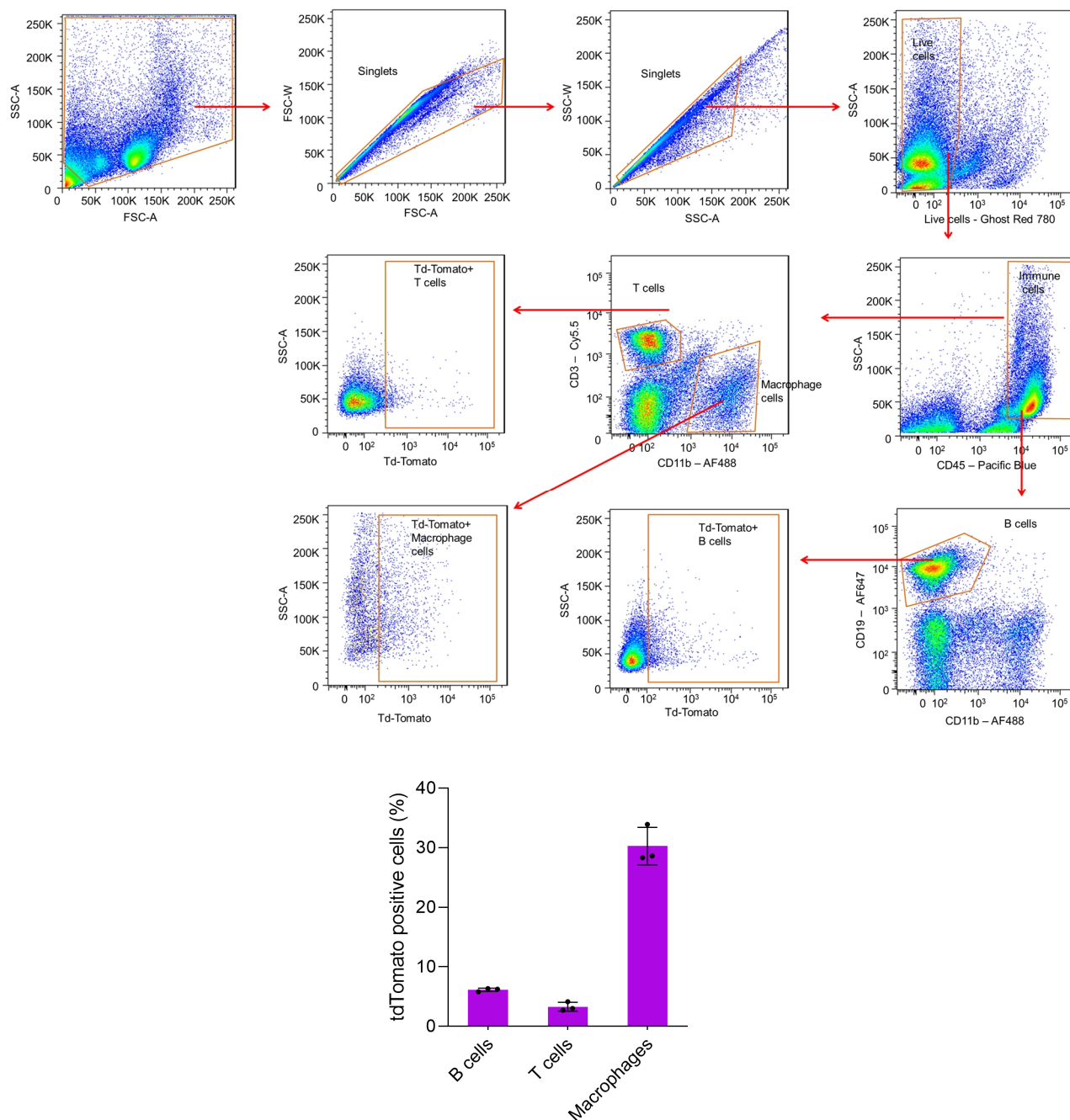


Supplementary Figure 25 | The FACS gating strategy for analysis of tdTomato expression in lung cells. Ghost Red 780 was utilized to distinguish live and dead cells. EpCam+ was used to define epithelial cells, CD45+ and CD31- were used to define immune cells, and CD45- and CD31+ were used to define endothelial cells. Gates for tdTomato+ in cell types were drawn based on PBS injected control Ai9 mice. Ai9 mice were IV injected by 9A1P9-DDAB iPLNPs (Cre mRNA, 0.25 mg kg⁻¹) and tdTomato+ in given cell types was detected by flow cytometry after 48 h. Data are presented as mean ± s.d. (n = 3 biologically independent mice).

PBS (spleen)

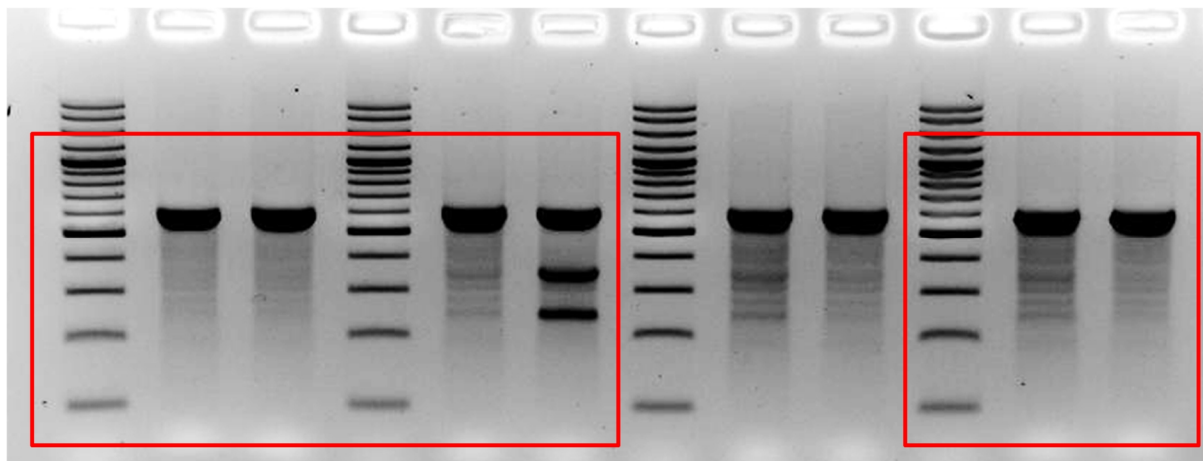


10A1P16-MDOA (spleen)

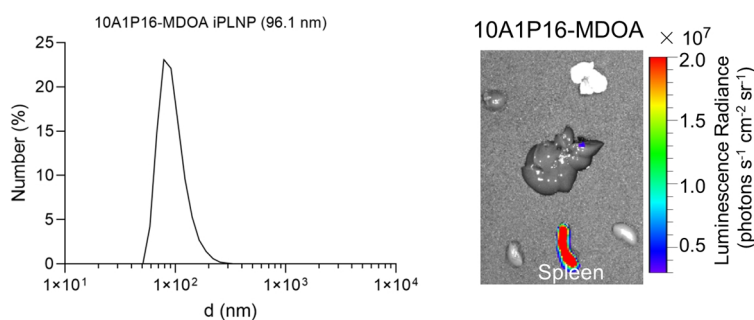


Supplementary Figure 26 | The FACS gating strategy for analysis of tdTomato expression in splenic cells. Ghost Red 780 was utilized to distinguish live and dead cells. CD45⁺ was used to distinguish immune cells, then CD3⁺ and CD11b⁻ were used for T cells, CD3⁻ and CD11b⁺ were used for macrophage cells, and CD19⁺ and CD11b⁻ were used for B cells. Gates for tdTomato⁺ in cell types were drawn based on PBS injected control mice. Ai9 mice were IV injected by 10A1P16-MDOA iPLNPs (Cre mRNA, 0.5 mg kg⁻¹) and tdTomato⁺ in given cell types was detected by flow cytometry after 48 h. Data are presented as mean ± s.d. (n = 3 biologically independent mice).

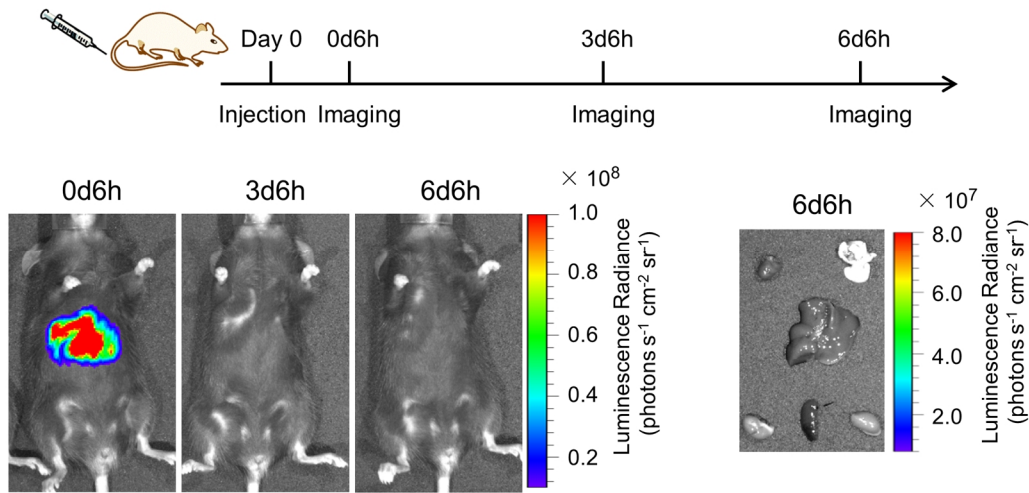
Fig. 6f (T7E1 for PTEN)



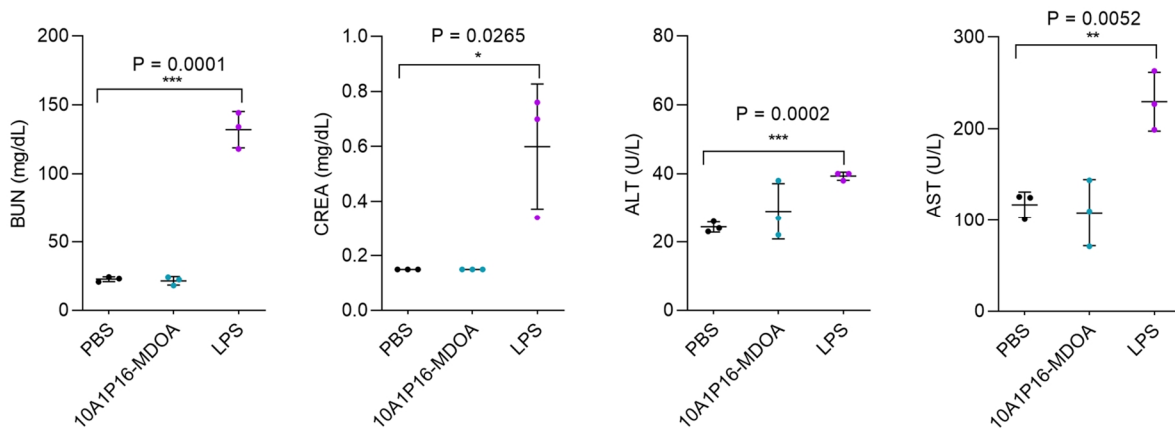
Supplementary Figure 27 | Uncropped original gel scans.



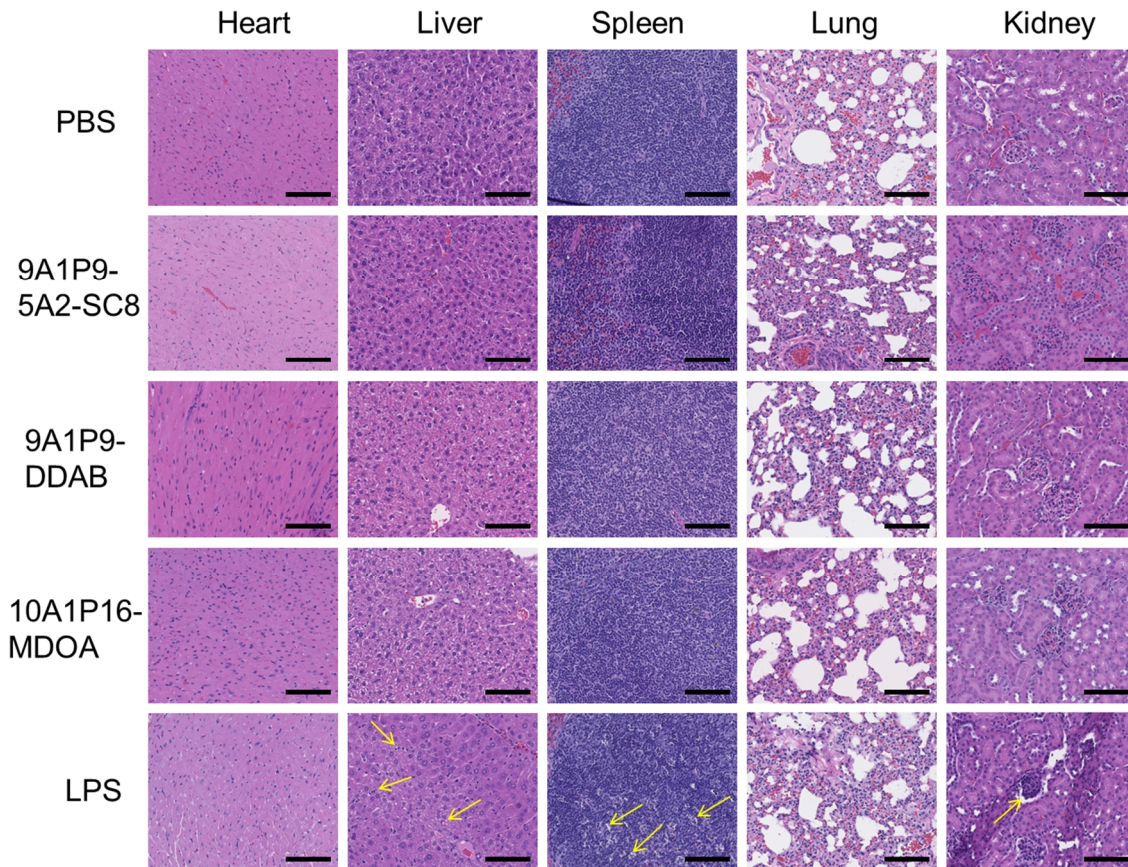
Supplementary Figure 28 | The NanoAssemblr microfluidic mixing system can be used to decrease iPLNP size. 10A1P16-MDOA iPLNPs were prepared using the NanoAssemblr microfluidic mixing system, demonstrating small size below 100 nm. High *in vivo* mRNA delivery efficacy and precise organ selectivity were fully retained after decreasing iPLNP diameters. 10A1P16-MDOA iPLNPs (Fluc mRNA, 0.25 mg kg⁻¹) mediated mRNA translation in the spleen (n = 3 biologically independent mice).



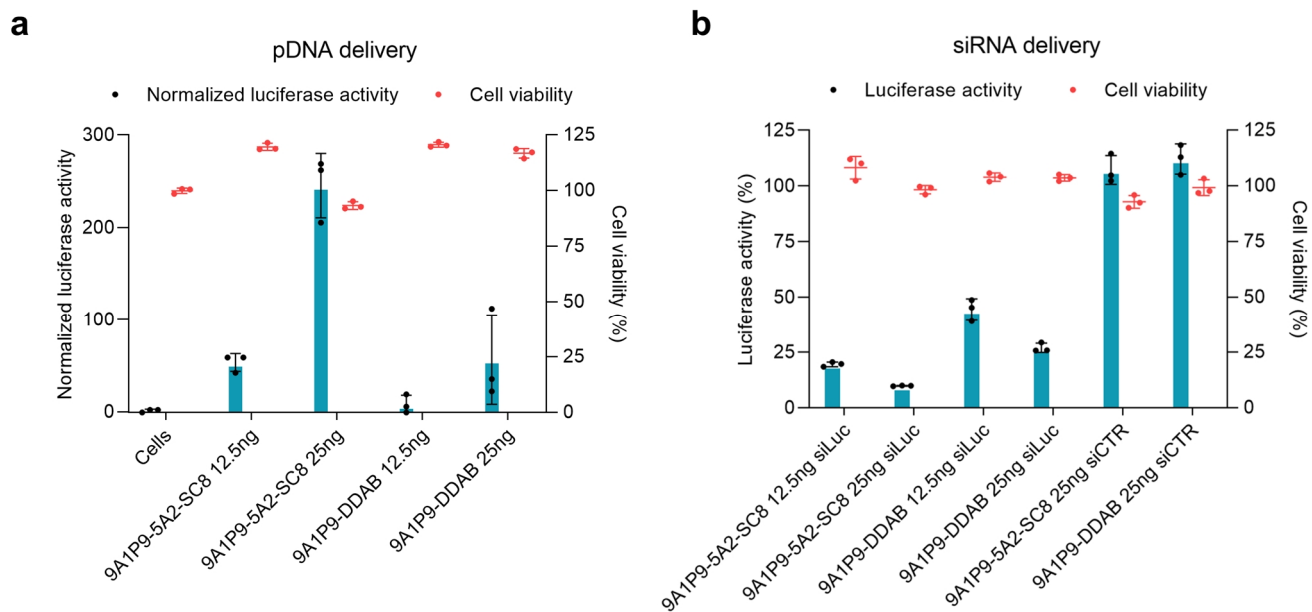
Supplementary Figure 29 | Control experiments confirm that Luciferase activity is short lived. To confirm that luciferase expression was short lived, we performed a control experiment where we examined late time points following a single administration ($n = 3$ biologically independent mice). Following single dosing of 9A1P9-5A2-SC8 iPLNPs, no efficacy was observed after 3 days 6 hours and 6 days 6 hours. As expected for a single administration, protein expression decreased over time and was not visible at later time points. This data supports the result of **Fig. 6i,j**.



Supplementary Figure 30 | 10A1P16-MDOA iPLNPs loading mRNA are well tolerated *in vivo*. 10A1P16-MDOA (spleen specific) iPLNPs were administrated intravenously (IV) to C57BL/6 mice (0.25 mg kg^{-1}). Lipopolysaccharide (LPS, 5 mg kg^{-1} , IP) was used as the positive control and PBS (IV) was examined as the negative control. 24 h post injection, kidney function (BUN and CREA) and liver function (ALT and AST) were evaluated. LPS treated mice showed severe kidney and liver injury. There was no significant difference between the 10A1P16-MDOA iPLNP and PBS groups. Data are presented as mean \pm s.d. ($n = 3$ biologically independent mice). Statistical significance was analyzed by the two-tailed unpaired t-test: ****, $P < 0.0001$; ***, $P < 0.001$; **, $P < 0.01$; *, $P < 0.05$.



Supplementary Figure 31 | Liver, lung, and spleen specific iPLNPs loading mRNA are well tolerated *in vivo*. 9A1P9-5A2-SC8 (liver specific), 9A1P9-DDAB (lung specific), and 10A1P16-MDOA (spleen specific) iPLNPs were administrated intravenously (IV) to C57BL/6 mice at a mRNA dose higher or equal to required for inducing high protein expression (0.25 mg kg^{-1} , $n = 3$ biologically independent mice). Lipopolysaccharide (LPS, 5 mg kg^{-1} , IP) was used as the positive control and PBS (IV) was examined as the negative control. 24 h post injection, tissue sections of heart, liver, spleen, lung, and kidney were prepared for H&E staining. LPS treated mice exhibited significant injury in multiple organs (arrows indicated), but iPLNP group mice showed no obvious injury. Scale bar = 100 μm .



Supplementary Figure 32 | iPLNPs enable efficient delivery of pDNA and siRNA. **a**, 9A1P9-5A2-SC8 iPLNPs and 9A1P9-DDAB iPLNPs were used to deliver pCMV-Luc pDNA. 12.5 ng and 25 ng pDNA per well were applied. The results were normalized to untreated cells. **b**, 9A1P9-5A2-SC8 iPLNPs and 9A1P9-DDAB iPLNPs efficiently delivered siLuc (siRNA). 12.5 ng and 25 ng siRNA per well were utilized. Data are presented as mean \pm s.d. (n = 3 biologically independent samples).

Supplementary Tables

Supplementary Table 1 | iPLNP compositions and ratios for organ selective mRNA expression.

Helper lipid	Molar ratios				9A1P9/mRNA (w/w)
	9A1P9	Helper lipid	Chol	DMG-PEG2000	
DOPE	55	30	45	0.2	18/1
MDOA	25	30	30	1	18/1
DODAP	25	30	30	1	18/1
5A2-SC8	25	30	30	1	18/1
DDAB	60	30	40	0.4	18/1
DOTAP	60	30	40	0.4	18/1

Supplementary Table 2 | sgRNA sequences used in this research.

Name	Target Sequences (5' to 3')	PAM (5' to 3')
sgTom 1	AAGTAAAACCTCTACAAATG	TGG
sgPTEN	AGATCGTTAGCAGAAACAAA	AGG

Supplementary Table 3 | PCR primers used in this research.

Name	Sequence (5' to 3')	Length	Purpose
PTEN_Forward	AAGCAGGCCCGAGTCTCTG	582 bp	For T7E1 assay
PTEN_Reverse	GACGAGCTCGCTAATCCAGTG		

Supplementary Methods

pKa determination using the 2-(p-toluidino)-6-naphthalenesulfonic acid (TNS) assay

The pKa of each iPLNP was determined by TNS assay. The iPLNPs comprised of synthetic iPhos/MDOA/chol/DMG-PEG2000 (25/30/30/1 mol%) were formulated in PBS at a concentration of 0.6 mM total lipid. TNS was prepared as a 100 μ M stock solution in milliQ water. The nanoparticles were diluted to 6 μ M total lipid in 100 μ L volume per well in 96-well plates with buffer solutions containing 10 mM 4-(2-hydroxyethyl)-1-piperazineethanesulfonic acid (HEPES), 10 mM 4-morpholineethanesulfonic acid (MES), 10 mM ammonium acetate and 130 mM sodium chloride (NaCl), where the pH ranged from 2.5 to 11. The TNS stock solution was added into each well to give a final concentration of 5 μ M. Afterward, the plate was read using excitation and emission wavelength of 321 nm and 445 nm, respectively. A sigmoidal fit analysis was applied to the fluorescence data and the pKa was measured as the pH giving rise to half-maximal fluorescence intensity.

iPLNP dissociation by fluorescence resonance energy transfer (FRET) assay

iPLNP dissociation was measured by mixing iPLNPs and endosomal mimicking anionic liposomes. The DOPE-conjugated FRET probes NBD-PE and Rho-PE were formulated into the same iPLNP. iPLNPs were prepared using iPhos: MDOA: chol: DMG-PEG2000: NBD-PE: Rho-PE lipid mixtures (molar ratio 25:30:30:1:0.86:0.86), with a final total lipid concentration of 1 mM. Other procedures were the same as the *in vitro* iPLNP formulation method. Endosomal mimicking anionic liposomes were prepared by mixing DOPS: DOPC: DOPE (molar ratio 25:25:50) in chloroform, followed by rotary evaporation and another 2 h vacuum dry to give a thin lipid film. The dried film was subsequently hydrated in PBS (pH 7.4), sonicated for 20 min and total lipid concentration was fixed at 10 mM. PBS (pH 5.5) was added to black 96-well plates (100 μ L/well), and 1 μ L iPLNPs were added to each well. Then 1 μ L endosomal mimicking anionic liposomes were added to the wells. After incubating at 37 $^{\circ}$ C for 10 min (or other noted time intervals), fluorescence measurements (F) were conducted on a microplate reader at Ex/Em = 465/520 nm. iPLNPs (with NBD-PE and Rho-PE inside) in PBS were set as negative control (F_{\min}). iPLNPs (with NBD-PE and Rho-PE inside) incubated with Triton X-100 solutions (2 wt. %) were set as positive control (F_{\max}). The iPLNP dissociation (%) was calculated as $(F - F_{\min}) / (F_{\max} - F_{\min}) * 100\%$.

Cell culture

Human ovarian adenocarcinoma cells (IGROV1, ATCC) were cultured in RPMI-1640 medium with 10% FBS and 1% Penicillin/Streptomycin (P/S). Human cervical cancer cells (Hela, ATCC) stably expressing firefly luciferase were cultured in Dulbecco's modified Eagle's medium (DMEM) with 10% FBS and 1% P/S. Cells were cultured at 37 $^{\circ}$ C and 5% CO₂ in a humidified atmosphere.

Animal experiments

All experiments were approved by the Institutional Animal Care and Use Committees of The University of Texas Southwestern Medical Center and were consistent with local, state, and federal regulations as applicable. Mice were maintained in a barrier facility with a 12-h light/12-h dark cycle, at 20 ~ 26 $^{\circ}$ C (average around 22 $^{\circ}$ C) and 30% ~ 60% humidity (average around 50%). Female C57BL/6 mice were

purchased from the UT Southwestern animal breeding core. B6.Cg-*Gt(ROSA)26Sor^{tm9(CAG-tdTomato)Hze}/J* mice (also known as Ai9 or Ai9(RCL-tdT) mice) were obtained from The Jackson Laboratory (007909) and bred to maintain homozygous expression of the Cre reporter allele that has a LoxP-flanked STOP cassette preventing transcription of a CAG promoter-driven red fluorescent tdTomato protein. Following Cre-mediated recombination, Ai9 mice will express tdTomato fluorescence. Ai9 mice are congenic on the C57BL/6J genetic background.

***In vivo* biodistribution**

Nanoparticles containing Cy5-labeled Fluc mRNA (Cy5-mRNA, 0.25 mg kg⁻¹) were prepared as *in vivo* iPLNP formulation method. iPLNPs were administered to female C57BL/6 mice (6-8 week old) *via* IV injection. 6 h later, mice were sacrificed, and the organs were isolated and imaged on the IVIS Spectrum *in vivo* imaging system (Perkin Elmer).

***In vivo* toxicity assay**

iPLNPs loading Fluc mRNA were prepared as *in vivo* iPLNP formulation method. 9A1P9: 5A2-SC8: chol: DMG-PEG2000 (molar ratio) of 25:30:30:1, 9A1P9: DDAB: chol: DMG-PEG2000 (molar ratio) of 60:30:40:0.4 and 10A1P16: MDOA: chol: DMG-PEG2000 (molar ratio) of 25:30:30:1 were used for 9A1P9-5A2-SC8 iPLNP (liver specific), 9A1P9-DDAB iPLNP (lung specific), and 10A1P16-MDOA iPLNP (spleen specific) formulation, respectively. All iPLNPs were IV administrated to C57BL/6 mice at a mRNA dose (0.25 mg kg⁻¹) higher to or equal to the requirement for inducing high protein expression. As controls, lipopolysaccharide (LPS, 5 mg kg⁻¹) was intraperitoneal (IP) administrated (the positive control), and PBS was IV administrated (the negative control). 24 h post administration, the whole blood was collected into BD Microtainer tubes, and serum was separated. The renal function (BUN and CREA) and liver function (ALT and AST) were evaluated in the UT Southwestern Metabolic Phenotyping Core. Tissue sections (heart, liver, spleen, lung and kidney) and H&E staining were conducted at the UT Southwestern Tissue Management shared resource. Slides were scanned with NDP.scan software version 3.1.9 (NANOZOOMER, Hamamatsu), and analyzed with NDP.view 2 software (version 2.7.25, Hamamatsu).

***In vivo* Cre mRNA delivery**

Nanoparticles containing Cre mRNA were prepared as *in vivo* iPLNP formulation method. Afterward, the nanoparticles were administered to Ai9 mice *via* IV injection. 48 h later, mice were sacrificed, and the organs were isolated and imaged on the IVIS Spectrum *in vivo* imaging system (Perkin Elmer).

Cell isolation for flow cytometry

Flow cytometry was used to determine the tdTomato positive cells in different cell types of various organs. Ai9 mice were IV administrated by iPLNPs containing Cre mRNA, and 48 h later, cell isolation and staining was conducted.

Hepatocytes were isolated using a two-step collagenase perfusion. The mice were anesthetized by isofluorane and fixed. Then perfusion was performed with liver perfusion medium (Thermo Fisher, 17701038) for 7-10 min, and followed by liver digestion medium (Thermo Fisher, 17703034) for another 7-10 min. Liver was cut to release the hepatocytes in liver digestion medium (10 mL), and the hepatocytes were washed with cold hepatocyte wash medium (Thermo Fisher, 17704024) and collected

by centrifugation (low speed, 50 g, 5 min). The cell pellet was resuspended in cold hepatocyte wash medium, and passed through a 100 μm filter. Then, the hepatocytes were washed twice more using cold hepatocyte wash medium, once with 1 \times PBS and passed through the 100 μm filter again. The hepatocytes were collected by centrifugation (50 g, 5 min), and analyzed with the fluorescence-activated cell sorting (FACS) Aria II SORP machine (BD FACSDiva software version 8.0.1, BD Biosciences).

For spleen cell isolation and staining, the collected spleen was minced and homogenized in 1 \times digestion medium (250 μL , 45 units μL^{-1} collagenase I, 25 units μL^{-1} DNase I and 30 units μL^{-1} hyaluronidase). The mixture was transferred to a 15 ml tube containing 1 \times digestion medium (10 mL). Then the mixture was passed through a 70 μm filter and washed with 1 \times PBS. After centrifugation (300 g, 5 min, 4 $^{\circ}\text{C}$), the cells were collected. Afterward, the cells were resuspended in 1 \times red blood cell lysis buffer (2 mL, BioLegend, 420301) and incubated on ice for 5 min. Cell staining buffer (4 mL, BioLegend) was then added to stop the red blood cell lysis. The mixture was centrifuged (300 g, 5 min) and the obtained pellet was resuspended in cell staining buffer. The cells and antibodies were transferred to flow tubes (100 μL), following incubation for 20 min at 4 $^{\circ}\text{C}$ in the dark. Then the cells were washed twice using 1 \times PBS, and resuspended in 1 \times PBS (500 μL) for final analysis. The antibodies, Alexa Fluor 488 anti-mouse/human CD11b (1/1600 dilution, BioLegend, 101217), Pacific Blue anti-mouse CD45 (1/200 dilution, BioLegend, 103126), PerCP-Cyanine5.5 anti-mouse CD3e (145-2C11) (1/40 dilution, Tonbo Biosciences, 65-0031) and Alexa Fluor 647 anti-mouse CD19 (1/400 dilution, BioLegend, 115522) were used here. Ghost Dye Red 780 (Tonbo Biosciences, 13-0865-T500) was utilized to discriminate live cells. Ultimately, the spleen cells were analyzed with the LSRForessa SORP machine (BD Biosciences).

For lung cell isolation and staining, the collected lung was minced and added in a 15 ml tube containing 2 \times digestion medium (10 mL, 90 units μL^{-1} collagenase I, 50 units μL^{-1} DNase I and 60 units μL^{-1} hyaluronidase). The mixture was incubated for 1 h at 37 $^{\circ}\text{C}$ under shaking. Afterward, the remaining lung tissue was homogenized. The remaining procedures were the same as above spleen protocol. The antibodies, Alexa Fluor 488 anti-mouse CD31 (1/800 dilution, BioLegend, 102414), Pacific Blue anti-mouse CD45 (1/400 dilution, BioLegend, 103126) and Alexa Fluor 647 anti-mouse CD326 (Ep-CAM) (1/1600 dilution, BioLegend, 118212) were used here. Ghost Dye Red 780 was utilized to discriminate live cells. Ultimately, the lung cells were analyzed with above LSRForessa SORP machine. These data were analyzed with FLOWJO software version 7.6 (FLOWJO).

DNA and siRNA delivery by iPLNPs

For DNA delivery, IGROV1 cells were seeded at a density of 1×10^4 cells per well in white opaque 96-well plates. 24 h later, 9A1P9-5A2-SC8 iPLNPs and 9A1P9-DDAB iPLNPs containing pCMV-luc DNA were prepared. Afterward, 150 μL fresh cell culture media were utilized to replace the previous media, and the formulated iPLNPs were added into the cells. 12.5 ng and 25 ng DNA per well was used. Post 48 h incubation, luciferase expression and cell viability were evaluated with the ONE-Glo + Tox luciferase assay kits.

For siRNA delivery, HeLa cells stably expressing firefly luciferase (HeLa-Luc) were seeded at a density of 1×10^4 cells per well in white opaque 96-well plates. 24 h later, 9A1P9-5A2-SC8 iPLNPs and 9A1P9-DDAB iPLNPs containing siRNA were formulated. Then, 150 μL fresh cell culture media were used to replace the previous media, and the iPLNPs were added into the cells. 12.5 ng and 25 ng siRNA per well was used. Post 24 h incubation, luciferase expression and cell viability were evaluated by the ONE-Glo + Tox luciferase assay kits.

The sequences for the sense and antisense strands of siRNAs were as follows:

siLuc (siRNA against Luciferase). dT are DNA bases. All others are RNA bases.

sense: 5'-GAUUAUGUCCGGUUAUGUA[dT][dT]-3'
antisense: 3'-UACAUAACCGGACAUAUAUC[dT][dT]-5'
siCTR (siRNA as control).
sense: 5'-GGAUCAUCUCAAGUCUUAC[dT][dT]-3'
antisense: 3'-GUAAGACUUGAGAUGAUCC[dT][dT]-5'

Statistical analyses

Statistical analyses were performed using GraphPad Prism version 8 (GraphPad Software). Two-tailed unpaired Student's t-test was used to determine the significance of the indicated comparisons. Data are expressed as mean \pm s.d. P-values < 0.05 (*), $P < 0.01$ (**), $P < 0.001$ (***) and $P < 0.0001$ (****) were considered to be statistically significant.